arXiv:1511.06171v1 [math.NA] 19 Nov 2015

# A micro-macro acceleration method for the Monte Carlo simulation of stochastic differential equations

Kristian Debrabant[1], Giovanni Samaey[2] and Przemysław Zieliński[2*]

[1]Department of Mathematics and Computer Science, University of Southern Denmark
[2]Department of Computer Science, University of Leuven

November 20, 2015

**Abstract**

We present and analyze a micro-macro acceleration method for the Monte Carlo simulation of stochastic differential equations with separation between the (fast) time-scale of individual trajectories and the (slow) time-scale of the macroscopic function of interest. The algorithm combines short bursts of path simulations with extrapolation of a number of macroscopic state variables forward in time. The new microscopic state, consistent with the extrapolated variables, is obtained by a matching operator that minimizes the perturbation caused by the extrapolation. We provide a proof of the convergence of this method, in the absence of statistical error, and we analyze various strategies for matching, as an operator on probability measures. Finally, we present numerical experiments that illustrate the effects of the different approximations on the resulting error in macroscopic predictions.

## 1 Introduction

In many applications one considers a process modeled with a stochastic differential equation (SDE) while one is ultimately concerned with the evolution of the expectation of a certain function of interest. This is, for instance, the case in the micro-macro simulation of dilute solutions of polymers [44], the motivating example in this paper, where an SDE models the evolution of the configuration of each individual polymer driven by the flow field, and the observable is a non-Newtonian stress tensor. For this type of problem one often resorts to Monte Carlo simulation [7], i.e., the simulation of a large ensemble of realizations of the SDE, combined with ensemble averaging to obtain an approximation of the quantity of interest at the desired moments in time. The analysis of the numerical properties of Monte Carlo simulations include: studies on the weak convergence of explicit [1, 9, 13, 39, 40, 51, 58] and implicit [2, 10–12, 39, 41] time discretizations of SDEs, investigation of stability [5, 6, 24–26, 28, 60, 66, 67], and development of techniques for variance reduction [14, 22, 23, 52]. Due to possibly high computational cost a large class of methods bypass Monte Carlo simulation replacing it by an analytically derived approximate macroscopic model, which consists of a number of evolution equations for the macroscopic state variables, complemented with a constitutive equation for the observable of interest (as a function of these variables). See [27, 32, 36, 48, 49, 63] for derivations of macroscopic closures for FENE dumbbell models in polymeric flow. In [33] the authors propose a *quasi-equilibrium* approach for dilute solutions of polymers (based on thermodynamical considerations and applicable to general SDEs with additive noise), while papers [61, 70] present several algorithms for simulating the evolution of this model numerically.

MSC 2010: (Primary) 65C30, 60H35, 65C05; (Secondary) 65C20, 68U20, 94A17
Key words: accelerated Monte Carlo, entropy optimization, FENE dumbbells, micro-macro simulations, multi-scale modeling, stochastic differential equations
*Email: przemyslaw.zielinski@kuleuven.be

We present and analyze a *micro-macro acceleration technique* for the Monte Carlo simulation of SDEs, motivated by the development of generic multi-scale techniques, such as *equation-free* [37, 38] and *heterogeneous multi-scale* methods [17, 18]. We consider an equation

$$\mathrm{d}\mathbf{X}(t) = \mathbf{a}(t, \mathbf{X}(t))\,\mathrm{d}t + \mathbf{b}(t, \mathbf{X}(t)) \star \mathrm{d}\mathbf{W}(t), \quad t \in [0, T], \tag{1.1}$$

in which $\mathbf{a}\colon [0,T] \times G \to \mathbb{R}^d$ is the drift vector, $\mathbf{b}\colon [0,T] \times G \to \mathbb{R}^{d\times m}$ is the dispersion matrix, $G \subseteq \mathbb{R}^d$ is open, and $\mathbf{W}$ is an $m$-dimensional Wiener process. As usual, (1.1) is an abbreviation of the integral form

$$\mathbf{X}(t) = \mathbf{X}(0) + \int_0^t \mathbf{a}(s, \mathbf{X}(s))\ \mathrm{d}s + \int_0^t \mathbf{b}(s, \mathbf{X}(s)) \star \mathrm{d}\mathbf{W}(s), \quad t \in [0, T]. \tag{1.2}$$

The integral with respect to $\mathbf{W}$ can be interpreted either as an Itô integral with $\star\,\mathrm{d}\mathbf{W} = \mathrm{d}\mathbf{W}$ or as a Stratonovich integral with $\star\,\mathrm{d}\mathbf{W} = \circ\,\mathrm{d}\mathbf{W}$. Equations (1.1) rsp. (1.2) are solved for given $\mathbf{X}(0)$ independent of $\mathbf{W}$. The function of interest for the Monte Carlo simulation is defined as the expectation $\mathbb{E}$ of a continuous function $\mathbf{g}\colon G \to \mathbb{R}^{d'}$ at time $t \in [0,T]$ via

$$t \mapsto \bar{\mathbf{g}}(t) = \mathbb{E}\mathbf{g}(\mathbf{X}(t)). \tag{1.3}$$

Our main interest lies in systems with a separation between a (fast) time-scale, on which individual trajectories of the SDE (1.1) need to be simulated, and a (slow) time-scale, on which the function of interest $\bar{\mathbf{g}}$ evolves.

We define the *microscopic* level via an ensemble $\mathscr{X} = (\mathbf{X}_j)_{j=1}^J$ of $J$ realizations evolving according to (1.1) and the *macroscopic* level via a vector of $L$ macroscopic state variables $\mathbf{m} = (\overline{R}_l)_{l=1}^L$, for some appropriately chosen functions $R_l$. The method exploits a separation in time scales by combining short bursts of *microscopic* simulation using SDE (1.1) with a *macroscopic* extrapolation step, in which only the macroscopic state $\mathbf{m}$ is extrapolated forward in time. One time step of the algorithm includes four stages: (1) microscopic *simulation* of the ensemble $\mathscr{X}$ using SDE (1.1); (2) *restriction*, i. e., extraction of an estimate of the macroscopic state (or macroscopic time derivative) based on simulation in the first stage; (3) forward in time *extrapolation* of the macroscopic state; and (4) *matching* of the ensemble that was available at the end of the microscopic simulation with the extrapolated macroscopic state. Here, the focus is precisely this matching step. In contrast with the numerical closures relying on the assumption that a closed model exists in terms of the macroscopic state variables, the micro-macro acceleration method only uses these variables for computational purposes, and maintains weak convergence to the full microscopic dynamics.

The main contributions of the present paper are the following:

- From a theoretical viewpoint, we propose and analyze a general framework for performing the matching step based on a *matching operator* that transforms a given prior distribution into a distribution consistent with a number of prescribed (extrapolated) macroscopic state variables, while introducing a "minimal perturbation" with respect to the prior. We make precise the notion of a "minimal perturbation" using different (semi-)distances between probability measures.
- From a numerical analysis viewpoint, we discuss how the resulting error depends on: the number $L$ of macroscopic state variables, the microscopic time discretization error, and the extrapolation time step. We prove the convergence of the micro-macro acceleration method in the absence of statistical error, i.e., without discretization in probability space, requiring only some general properties of the matching operator. We additionally show that these consistency properties are fulfilled for a specific matching operator based on the $L_2$-norm distance.
- From a practical viewpoint, we provide numerical results for a nontrivial test case. We discuss how to implement the different matching operators for ensembles of finite size, and illustrate the interplay between the different sources of numerical error.

Section 2 gives the precise mathematical setting and the motivating polymer problem. Section 3 describes the micro-macro acceleration method. Section 4 details some examples and analysis of matching operators. Section 5 provides the proof of convergence of the micro-macro method. Some numerical illustrations are given in Section 6 while Section 7 concludes with an outlook to future work.

# 2 Mathematical setting and model problems

## 2.1 Preliminaries

Throughout the paper we denote by: $\mathbb{N} = \{1, 2, \ldots\}$ the set of natural numbers; $\mathbb{N}_0$ the set of positive integers $\{0\} \cup \mathbb{N}$; $\mathbb{R}^d$, for $d \in \mathbb{N}$, the $d$-dimensional Euclidean space with 2-norm $\|\cdot\|$; $\mathbb{R} = \mathbb{R}^1$. For any multi-index $\alpha = (\alpha_1, \ldots, \alpha_d) \in \mathbb{N}_0^d$ and $\mathbf{x} = (x_1, \ldots, x_d) \in \mathbb{R}^d$ by $\partial_{\mathbf{x}}^{\alpha}$ we mean the partial derivative $\partial_{x_1}^{\alpha_1} \ldots \partial_{x_d}^{\alpha_d}$ of order $|\alpha| = \alpha_1 + \ldots + \alpha_d$.

### 2.1.1 Notations and assumptions on the SDE

We consider the SDE (1.1) on the time interval $I = [0, T]$, with $T > 0$. We will need to compare solutions starting from different initial conditions at different moments in time. To keep track of these solutions, we denote by $\mathbf{X}(\,\cdot\,; t, \mathbf{Z})$ the solution of the auxiliary problem

$$\mathbf{X}(s; t, \mathbf{Z}) = \mathbf{Z} + \int_t^s \mathbf{a}(u, \mathbf{X}(u; t, \mathbf{Z}))\,\mathrm{d}u + \int_t^s \mathbf{b}(u, \mathbf{X}(u; t, \mathbf{Z})) \star \mathrm{d}\mathbf{W}(u) \tag{2.1}$$

on the interval $[t, T]$, with $0 \le t \le T$ and $\mathbf{Z}$ a given random variable independent of $\{\mathbf{W}(s)\}_{s \ge t}$. We will always assume, without explicitly mentioning, that the initial condition $\mathbf{Z}$ has values a.s. in $G$, i.e., $\mathbb{P}(\mathbf{Z} \in G) = 1$, and that (2.1) has unique strong solutions up to time $T$ for all such initial conditions $\mathbf{Z}$. Moreover, we will also assume that the algebraic moments $\mathbb{E}\|\mathbf{X}(s; t, \mathbf{Z})\|^r = \mathbb{E}[\|\mathbf{X}(s; t, \mathbf{Z})\|^r]$ exist for all $r \in \mathbb{N}$, if this is the case for $\mathbf{Z}$.

We are interested in the evolution of functionals of the form (1.3), for specific functions of interest $g\colon G \to \mathbb{R}$. We first define the appropriate function class suitable for our analysis. Let $C_P^r(G, \mathbb{R})$ denote the space of all functions[1] $g \in C^r(G, \mathbb{R})$ that can be (together with all their partial derivatives) polynomially bounded, i.e., for which there exist constants $C > 0$ and $\kappa > 0$ such that $|\partial_{\mathbf{x}}^{\alpha} g(\mathbf{x})| \le C(1 + \|\mathbf{x}\|^{2\kappa})$ for all $|\alpha| \le r$ and $\mathbf{x} \in G$. Further, we write $g \in C_P^{q,r}(I \times G, \mathbb{R})$ if $g(\cdot, \mathbf{x}) \in C^q(I, \mathbb{R})$, $g(t, \cdot) \in C^r(G, \mathbb{R})$ for all $t \in I$, $\mathbf{x} \in G$, and $|\partial_t^i \partial_{\mathbf{x}}^{\alpha} g(t, \mathbf{x})| \le C(1 + \|\mathbf{x}\|^{2\kappa})$ holds for all $0 \le i \le q$, $|\alpha| \le r$ and $\mathbf{x} \in G$, uniformly with respect to $t \in I$ (cf. [39, p. 153], [51, Def. 8.1., p. 102]).

We are now ready to state the main assumptions on the class of SDEs that we consider.

**Assumption 2.1.** *Let $g \in C_P^{2(p+1)}(G, \mathbb{R})$ with some $p \in \mathbb{N}_0$.*

*a. For every $t \in [0, T)$ the function $(s, \mathbf{z}) \mapsto \mathbb{E}g\big(\mathbf{X}(s; t, \mathbf{z})\big)$ belongs to $C_P^{p+1,0}([t, T] \times G, \mathbb{R})$ with constants $C$ and $\kappa$ uniform also with respect to $t$.*

*b. For every $s \in (0, T]$ the function $(t, \mathbf{z}) \mapsto \mathbb{E}g\big(\mathbf{X}(s; t, \mathbf{z})\big)$ belongs to $C_P^{0,2(p+1)}([0, s] \times G, \mathbb{R})$ with constants $C$ and $\kappa$ uniform also with respect to $s$.*

*c. There is a constant $C_{g,T} > 0$ such that for every $0 \le t \le s \le T$ and any initial random variables $\mathbf{Z}_1, \mathbf{Z}_2$:*

$$\big|\mathbb{E}g\big(\mathbf{X}(s; t, \mathbf{Z}_1)\big) - \mathbb{E}g\big(\mathbf{X}(s; t, \mathbf{Z}_2)\big)\big| \le C_{g,T} |\mathbb{E}g(\mathbf{Z}_1) - \mathbb{E}g(\mathbf{Z}_2)|.$$

Assumption 2.1.a corresponds to the existence of stochastic Taylor expansion (w.r.t. increments of the time) of the expectation of the functions of interest, which is essential for constructing extrapolation with appropriate order of consistency (cf. Lemma 3.8). For the proof of convergence of such expansions and the analysis of truncation error see [59]. Assumption 2.1.b ensures that the functions of interest remain polynomially bounded under the evolution of the SDE (1.1) and is satisfied, for instance, when $\mathbf{a} \in C_P^{2(p+1)}(\mathbb{R}^d, \mathbb{R}^d)$ and $\mathbf{b} \in C_P^{2(p+1)}(\mathbb{R}^d, \mathbb{R}^{d \times m})$ [39, Thm. 4.8.6, p. 153]. Finally, we can look at Assumption 2.1.c as a particular kind of weak continuous dependence on the initial condition.

[1] When writing $C^r(G, \mathbb{R})$, we mean the space of functions from $G$ to $\mathbb{R}$ which have continuous partial derivatives up to order $r \ge 0$.

We finish this section with one immediate consequence of Assumption 2.1.a.

**Lemma 2.2.** *For every $g \in C_P^2(G,\mathbb{R})$ there are constants $C_{g,T}$ and $\kappa_{g,T}$ such that for all $0 \le t \le s \le T$ and any initial random variable $\mathbf{Z}$ it holds*

$$\left|\mathbb{E}g\big(\mathbf{X}(s;t,\mathbf{Z})\big)\right| \le C_{g,T}(1+\mathbb{E}\|\mathbf{Z}\|^{2\kappa_{g,T}}).$$

*In particular, all moments $\mathbb{E}\|\mathbf{X}(s;t,\mathbf{Z})\|^{2r}$ remain uniformly bounded with respect to $t$ and $s$.*

*Proof.* Let us fix $t \in [0,T)$ and denote $v(s,\mathbf{z}) = \mathbb{E}g\big(\mathbf{X}(s;t,\mathbf{z})\big)$, $(s,\mathbf{z}) \in [t,T]\times G$. If $C$ and $\kappa$ are the constants from Assumption 2.1.a, we get employing mean value theorem

$$|v(s,\mathbf{z}) - v(t,\mathbf{z})| \le \max_{u\in[t,s]} |\partial_u v(u,\mathbf{z})| \cdot (s-t) \le C(1+\|\mathbf{z}\|^{2\kappa})\cdot(s-t).$$

Hence, $|\mathbb{E}v(s,\mathbf{Z}) - \mathbb{E}v(t,\mathbf{Z})| \le C(1+\mathbb{E}\|\mathbf{Z}\|^{2\kappa})\cdot(s-t)$, by monotonicity of expected value, and from the definition of $v$ we obtain

$$\left|\mathbb{E}g\big(\mathbf{X}(s;t,\mathbf{Z}) - \mathbb{E}g\big(\mathbf{Z}\big)\right| \le C(1+\mathbb{E}\|\mathbf{Z}\|^{2\kappa})\cdot(s-t), \tag{2.2}$$

where $C$ and $\kappa$ depend only on $g$ and $T$. Consequently we have

$$\begin{aligned}\left|\mathbb{E}g\big(\mathbf{X}(s;t,\mathbf{Z})\big)\right| &\le \left|\mathbb{E}g\big(\mathbf{X}(s;t,\mathbf{Z}) - \mathbb{E}g\big(\mathbf{Z}\big)\right| + \left|\mathbb{E}g\big(\mathbf{Z}\big)\right| \le \\ &\le CT(1+\mathbb{E}\|\mathbf{Z}\|^{2\kappa}) + \widetilde{C}(1+\mathbb{E}\|\mathbf{Z}\|^{2\widetilde{\kappa}}) \le C_{g,T}(1+\mathbb{E}\|\mathbf{Z}\|^{2\kappa_{g,T}}),\end{aligned}$$

where $\widetilde{C}$ and $\widetilde{\kappa}$ come from the definition of the space $C_P$ and we put $C_{g,T} = 2(CT+\widetilde{C})$, $\kappa_{g,T} = \kappa + \widetilde{\kappa}$. □

### 2.1.2 Notations and assumptions on time discretization

Let $\delta t > 0$ and let $\boldsymbol{\xi} \in \mathbb{R}^m$ be a vector of $m$ independent standard normal random variables, representing the increment of the $m$-dimensional Wiener process $\mathbf{W}$ over a time interval of length one. We denote a generic one-step time discretization method approximating the solution $\mathbf{X}(t+\delta t;t,\mathbf{Z})$ of (2.1) as

$$S(t,\mathbf{Z};\delta t,\boldsymbol{\xi}). \tag{2.3}$$

Since, in the Monte Carlo setting, we are interested in the weak approximation, we require $S$ to satisfy the following definition (compare [51, p. 113]).

**Definition 2.3** (Weak consistency of SDE discretization)**.** If for all $g \in C_P^{2(p_S+1)}(G,\mathbb{R})$ there exists a $C_{g,T} \in C_P^0(G,\mathbb{R})$ such that

$$\left|\mathbb{E}g\big(S(t,\mathbf{z};\delta t,\boldsymbol{\xi})\big) - \mathbb{E}g\big(\mathbf{X}(t+\delta t;t,\mathbf{z})\big)\right| \le C_{g,T}(\mathbf{z})\cdot(\delta t)^{p_S+1}$$

is valid for all $\mathbf{z} \in G$ and $t$, $t+\delta t \in I$, we call the one-step method $S$ *weakly consistent of order* $p_S$.

To discretize SDE (2.1) over the interval $[t^0,t^K] \subseteq I$ with $K \in \mathbb{N}$ uniform steps, we let $\delta t = (t^K - t^0)/K$ and put $t^k = t + k\delta t$ for $k = 0,\dots,K$. Moreover, we fix the sequence $(\boldsymbol{\xi}^k)_{k=1,\dots,K}$ of independent normally distributed random vectors in $\mathbb{R}^m$. We begin by taking $\mathbf{X}^0 = \mathbf{Z}$ and, assuming that $\mathbf{X}^k$ is given for $k < K$, we put

$$\mathbf{X}^{k+1} = S(t^k,\mathbf{X}^k;\delta t,\boldsymbol{\xi}^k,) \equiv S^k(\mathbf{X}^k;\delta t). \tag{2.4}$$

We require the sequences of random variables generated by $S$ to have moments uniformly bounded with respect to $K$. More precisely:

**Assumption 2.4.** *For every sufficiently large $r$ there is a constant $C_{r,T}$ such that, if $\mathbf{X}^k$ is given by (2.4), we have*

$$\mathbb{E}\|\mathbf{X}^k\|^{2r} \le C_{r,T}\mathbb{E}\|\mathbf{X}^0\|^{2r} \quad k = 1,\dots,K.$$

See for example [51, Lem. 9.1] for a sufficient condition on general one-step methods for this requirement, and [57, Proposition 6.2] in case of Runge-Kutta methods.

For the discretization on the whole interval $[t^0, t^K]$ we have, as a consequence of assumptions already made, the following property.

**Lemma 2.5.** *For all $g \in C_P^{2(p_S+1)}$ there are constants $C_{g,T}$ and $\kappa_{g,T}$ such that*

$$\left|\mathbb{E}g\big(\mathbf{X}(s;t^K,\mathbf{X}^K)\big) - \mathbb{E}g\big(\mathbf{X}(s;t^0,\mathbf{X}^0)\big)\right| \le C_{g,T}(1+\mathbb{E}\|\mathbf{X}^0\|^{2\kappa_{g,T}})\cdot K(\delta t)^{p_S+1},$$

*uniformly with respect to $s \in [t^K, T]$.*

*Proof.* Assumption 2.1.c provides us with a constant $\widetilde{C}_{g,T} > 0$ such that

$$\begin{aligned}\left|\mathbb{E}g\big(\mathbf{X}(s;t^K,\mathbf{X}^K)\big) - \mathbb{E}g\big(\mathbf{X}(s;t^0,\mathbf{X}^0)\big)\right| &\le \sum_{k=1}^{K}\left|\mathbb{E}g\big(\mathbf{X}(s;t^k,\mathbf{X}^k)\big) - \mathbb{E}g\big(\mathbf{X}(s;t^{k-1},\mathbf{X}^{k-1})\big)\right| \\ &\le \widetilde{C}_{g,T}\sum_{k=1}^{K}\left|\mathbb{E}g\big(\mathbf{X}^k\big) - \mathbb{E}g\big(\mathbf{X}(t^k;t^{k-1},\mathbf{X}^{k-1})\big)\right|,\end{aligned}$$

where we used the identity $\mathbf{X}(s;t^{k-1},\mathbf{X}^{k-1}) = \mathbf{X}(s;t^k,\mathbf{X}(t^k;t^{k-1},\mathbf{X}^{k-1}))$, valid due to the uniqueness of solutions. Moreover by Definition 2.3

$$\left|\mathbb{E}g\big(\mathbf{X}^k\big) - \mathbb{E}g\big(\mathbf{X}(t^k;t^{k-1},\mathbf{X}^{k-1})\big)\right| \le \mathbb{E}\overline{C}_{g,T}(\mathbf{X}^{k-1})(\delta t)^{p_S+1} \le \overline{C}(1+\mathbb{E}\|\mathbf{X}^{k-1}\|^{2\overline{\kappa}})(\delta t)^{p_S+1},$$

where $\overline{C}$ and $\overline{\kappa}$ are constants corresponding to function $\overline{C}_{g,T} \in C_P^0(G,\mathbb{R})$. Finally, for sufficiently large constants $r > \overline{\kappa}$ and $\widetilde{C}_{r,T} > 1$, independent of $K$, we can employ Assumption 2.4 to get $\mathbb{E}\|\mathbf{X}^{k-1}\|^{2\overline{\kappa}} \le 1 + \mathbb{E}\|\mathbf{X}^{k-1}\|^{2r} \le \widetilde{C}_{r,T}(1+\mathbb{E}\|\mathbf{X}^0\|^{2r})$ for every $k = 1,\dots,K$. □

In the Itô case, when $G = \mathbb{R}^d$ one can use the Euler-Maruyama scheme,

$$\mathbf{X}^{k+1} = \mathbf{X}^k + \mathbf{a}(t^k,\mathbf{X}^k)\delta t + \mathbf{b}(t^k,\mathbf{X}^k)\sqrt{\delta t}\boldsymbol{\xi}^k \tag{2.5}$$

which, for Lipschitz continuous coefficients, has weak order 1, see [39, 51]. In case that $G$ is bounded, we supplement this scheme with a truncation step (see Section 2.2.2).

### 2.1.3 Monte Carlo simulation

To discretize SDE (1.1) in probability space we employ Monte Carlo method [7], simulating a finite number $J$ of SDE realizations. Given a random variable $\mathbf{X}(t)$, the solution of (1.1) at time $t \in I$, we denote the realization corresponding to the event $\omega_j$ (that defines the specific Brownian path $t \mapsto \mathbf{W}(t;\omega_j)$) as $\mathbf{X}_j(t) \equiv \mathbf{X}(t;\omega_j)$.

For a given continuous function of interest $\mathbf{g}\colon \mathbb{R}^d \to \mathbb{R}^{d'}$ and the ensemble $\mathscr{X} = \{\mathbf{X}_j\}_{j=1}^J$, the Monte Carlo estimate of the expectation of $\mathbf{g}$ is

$$\hat{\mathbf{g}}(\mathscr{X}) = \frac{1}{J}\sum_{j=1}^{J}\mathbf{g}(\mathbf{X}_j).$$

We approximate the evolution of $\bar{\mathbf{g}}$, defined in (1.3), on $[t^0, t^K] \subseteq I$ with the sequence $\hat{\mathbf{g}}^k = \hat{\mathbf{g}}(\mathscr{X}^k)$, $k = 1,\dots,K$, where $\{\mathscr{X}^k\}_{k=1}^K$ is produced by the time discretization scheme (2.4) with uniform mesh $\{t^0, t^1, \dots t^K\}$. The total error of simulation consists of a deterministic or systematic error – due to the time discretization (quantified by the weak error of the scheme), and a statistical error – due to the finite number of samples. See [39] and references therein for more details on Monte Carlo simulation.

### 2.1.4 Probability density functions

For the analysis of the matching operator we will assume that, for every $t \in I = [0,T]$, the solution $\mathbf{X}(t)$ of (1.1) has a probability density function (PDF) $\rho(t,\cdot)$. In the Itô case this

density evolves according to an advection-diffusion equation, also known as Fokker-Planck equation,

$$\partial_t \rho = \nabla_{\mathbf{x}} \cdot \left( -\rho \mathbf{a} + \frac{1}{2} \nabla_{\mathbf{x}} \cdot (\rho\, \boldsymbol{\Sigma}) \right), \quad \text{on } (0,T) \times G, \tag{2.6}$$

where $\boldsymbol{\Sigma} = \mathbf{b}\mathbf{b}^T$ is the diffusion matrix. We supplement (2.6) with initial-boundary condition

$$\rho(0,\cdot) = \rho_0 \text{ on } G, \quad \rho(\cdot,\mathbf{x}) = 0 \text{ for every } \mathbf{x} \in \partial G \tag{2.7}$$

where $\rho_0$ is the law of $\mathbf{X}(0)$. It can be proved (under certain assumptions, see [54]) that for all $t \in I$ the solution $\rho(t,\cdot)$ of (2.6)–(2.7) is also a probability density. Hence, we can equivalently compute the averages in (1.3) as

$$\overline{\mathbf{g}}(t) = \int_G \mathbf{g}(\mathbf{x})\, \rho(t,\mathbf{x})\, \mathrm{d}\mathbf{x}, \quad t \in I. \tag{2.8}$$

Note that, for $G = \mathbb{R}^d$, the integral is finite for any $g \in C_P^0(G,\mathbb{R})$ when $\rho(t,\cdot)$ is decaying rapidly (i.e. faster than any polynomial) at infinity. Moreover, we can guarantee the higher regularity of the solutions to (2.6), this is related to Assumption 2.1, with appropriate smoothness of the initial condition $\rho_0$ and the coefficients $\mathbf{a}$ and $\mathbf{b}$ (see the discussion in Section 2.2.1 and [54])

## 2.2 Motivating problem: dilute solution of polymers

We consider a coupled micro-macro model for the evolution of a dilute solution of polymers immersed in a homogeneous fluid. We restrict ourselves to the simplest case – the so-called dumbbell model – where the polymer chain is represented by two beads linked by a spring. In this case, we describe the state of the polymer configuration at time $t \geq 0$ with the end-to-end (random) vector $\mathbf{X}(t) \in \mathbb{R}^d$ that connects both beads. Its evolution is modeled using the SDE (2.9d) that takes into account Stokes drag (due to the solvent velocity field), a spring force $\mathbf{F}$ (modeling intramolecular elastic forces) and Brownian motion (resulting from the collisions with solvent molecules). Finally, we couple this equation with the incompressible Navier-Stokes system (2.9a)-(2.9b) for the macroscopic flow via the stress tensor (2.9c). The complete model, in non-dimensional form, reads as follows:

$$\mathrm{Re}\big(\partial_t \mathbf{u} + (\mathbf{u}\cdot\nabla_{\boldsymbol{\zeta}})\mathbf{u}\big) = -\nabla_{\boldsymbol{\zeta}} p + (1-\varepsilon)\Delta_{\boldsymbol{\zeta}} \mathbf{u} + \mathrm{div}_{\boldsymbol{\zeta}}\, \boldsymbol{\tau}, \tag{2.9a}$$

$$\mathrm{div}_{\boldsymbol{\zeta}}\, \mathbf{u} = 0, \tag{2.9b}$$

$$\boldsymbol{\tau} = \frac{\varepsilon}{\mathrm{We}} (\mathbb{E}\left[\mathbf{X} \otimes \mathbf{F}(\mathbf{X})\right] - \mathbf{Id}), \tag{2.9c}$$

$$\mathrm{d}\mathbf{X} + \mathbf{u}\cdot\nabla_{\boldsymbol{\zeta}}\mathbf{X}\, \mathrm{d}t = \left[\nabla_{\boldsymbol{\zeta}}\mathbf{u}\cdot\mathbf{X} - \frac{1}{2\mathrm{We}}\mathbf{F}(\mathbf{X})\right] \mathrm{d}t + \frac{1}{\sqrt{\mathrm{We}}}\, \mathrm{d}\mathbf{W}, \tag{2.9d}$$

where $\mathbf{u} = \mathbf{u}(t,\boldsymbol{\zeta})$ is the velocity field of the fluid, $p = p(t,\boldsymbol{\zeta})$ is the pressure, $\boldsymbol{\tau} = \boldsymbol{\tau}(t,\boldsymbol{\zeta})$ is the stress tensor, and $\mathbf{X} = \mathbf{X}(t,\boldsymbol{\zeta})$ denotes the end-to-end vector of the polymer at time $t$ and sitting at the macro-point $\boldsymbol{\zeta}$ of the fluid. The parameters are the Reynolds number $\mathrm{Re} > 0$, the Weissenberg number $\mathrm{We} > 0$ and $\varepsilon > 0$ measuring the ratio of viscosity of the polymers over the total viscosity. We refer to [45] for the derivation of system (2.9) and the definition of the non-dimensional numbers Re, We and $\varepsilon$.

The calculation of polymer stress poses the most demanding task in the simulation of the coupled system (2.9), since we need to simulate an ensemble of realizations of the stochastic process (2.9d) in each mesh point of the spatial and temporal discretization. In the presence of a large time-scale separation between the (fast) evolution of individual realizations of SDE (2.9d) and the (slow) evolution of the stress tensor $\boldsymbol{\tau}$, the cost of this Monte Carlo simulation may quickly become prohibitive.

### 2.2.1 Microscopic FENE model

In this paper, we focus on the finitely extensible, nonlinearly elastic (FENE) entropic force, defined as

$$\mathbf{F}\colon B(\sqrt{b}) \to \mathbb{R}^d, \mathbf{x} \mapsto \mathbf{F}(\mathbf{x}) = \frac{b}{b - \|\mathbf{x}\|^2}\, \mathbf{x}, \tag{2.10}$$

where $B(\sqrt{b}) = \{\mathbf{x} \in \mathbb{R}^d : \|\mathbf{x}\|^2 < b\}$, with $b > 0$ a non-dimensional parameter that is related to the maximal polymer length. Note that $\mathbf{F} = \nabla U(\|\cdot\|)$ where

$$U(r) = -\frac{b}{4} \ln\left(1 - \frac{r^2}{b}\right), \quad r \in [0, \sqrt{b}), \tag{2.11}$$

is the FENE spring potential. We consider only the simulation of the microscopic model, leaving the coupling with the Navier-Stokes equations for future work. Thus, we assume that the velocity field of the solvent $\mathbf{u}$ is given, which makes equations (2.9a) and (2.9b) irrelevant. We eliminate the spatial dependence in equation (2.9d) using the characteristic method along the flow field, i.e., Lagrangian frame, to integrate the convective derivative. This results in the following SDE

$$\mathrm{d}\mathbf{X}(t) = \left(\boldsymbol{\kappa}(t)\mathbf{X}(t) - \frac{1}{2\mathrm{We}}\mathbf{F}(\mathbf{X}(t))\right)\mathrm{d}t + \frac{1}{\sqrt{\mathrm{We}}}\mathrm{d}\mathbf{W}(t), \quad t \in I = [0, T], \tag{2.12}$$

where the matrix-valued function $\boldsymbol{\kappa} \in C(I, \mathbb{R}^{d\times d})$ is the given time-dependent velocity gradient of the fluid along characteristics. Equation (2.12) is supplemented with the initial condition

$$\mathbf{X}(0) = \mathbf{X}^0 \ \text{ a.s. with } \ \mathbb{P}(\|\mathbf{X}^0\|^2 < b) = 1. \tag{2.13}$$

In [34, 35] the authors established the existence of the unique global solution to (2.12)–(2.13) in two space dimensions ($d = 2$) when the velocity gradient $\boldsymbol{\kappa}$ is unidirectional and of particular form $\boldsymbol{\kappa}(\cdot) = (\kappa_1(\cdot), 0)^T$. The trajectorial uniqueness is valid only when $b \geq 2$ and is guaranteed by the fact that the solution almost surely does not reach the boundary of $B(\sqrt{b})$.

For the FENE SDE (2.12), the corresponding Fokker-Planck equation (2.6) reads

$$\partial_t \rho = -\operatorname{div}_{\mathbf{x}}\left(\rho\left[\boldsymbol{\kappa}\,\mathbf{Id} - \frac{1}{2\mathrm{We}}\mathbf{F}\right]\right) + \frac{1}{2\mathrm{We}}\Delta_{\mathbf{x}}\rho, \quad \text{on } (0,T)\times B(\sqrt{b}). \tag{2.14}$$

In [31, 50] the authors provide requirements on the initial condition $\rho_0$ that ensure the well-posedness of the system (2.14)–(2.7) and regularity of its solutions, which is appropriate for our analysis. In particular, Theorem 1.2 in [31] implies that if $\boldsymbol{\kappa} \in C^\infty(I)$, $\rho_0 \in C^\infty(\overline{B})$ and

$$\partial_{\mathbf{x}}^\alpha(\rho_0 e^U) = 0 \text{ at } \partial B, \text{ for all } \alpha \in \mathbb{N}_0^d,$$

there exists a unique smooth solution to (2.14)–(2.7).

The function of interest for the Monte Carlo simulation is the stress tensor (2.9c). In the numerical tests in Section 6, we will further choose $\varepsilon = 1$ and $d = 1$, so that equations (2.12) and (2.9c) become scalar. In that case, we will not use bold symbols.

### 2.2.2 Time discretization

We will use the explicit Euler-Maruyama scheme (2.5), combined with an accept-reject (truncation) strategy. Scheme (2.5) takes the specific form

$$\widetilde{\mathbf{X}}^{k+1} = \mathbf{X}^k + \left(\boldsymbol{\kappa}(t^k)\mathbf{X}^k - \frac{1}{2\mathrm{We}}\mathbf{F}(\mathbf{X}^k)\right)\delta t + \frac{1}{\sqrt{\mathrm{We}}}\sqrt{\delta t}\boldsymbol{\xi}^k, \tag{2.15}$$

where we added a tilde on $\widetilde{\mathbf{X}}^{k+1}$ to emphasize that this is an intermediate result.

An accept-reject strategy is necessary because (2.15) might take the spring length out of the domain of definition, resulting in a random variable $\widetilde{\mathbf{X}}^{k+1}$ for which $\mathbb{P}(\|\widetilde{\mathbf{X}}^{k+1}\|^2 \geq b) > 0$. To avoid this, $\widetilde{\mathbf{X}}^{k+1}$ is rejected if $\|\widetilde{\mathbf{X}}^{k+1}\| > \alpha\sqrt{b}$, with $0 < \alpha \leq 1$, and accepted otherwise. Upon rejection, we repeat the step (2.15) using a different Brownian increment $\boldsymbol{\xi}^k$. On the one hand, the parameter $\alpha$ should be chosen carefully in order to maintain consistency; in particular $\alpha$ needs to tend to 1 as $\delta t$ tends to zero. On the other hand, with a finite time step, extensions very close to $\sqrt{b}$ produce a large displacement in the next step, and thus many rejections. In the numerical experiments, following [53, Sec. 4.3.2], we choose $\alpha = 1 - \sqrt{\delta t}$.

The introduction of the cut-off factor $\alpha \in (0,1)$ results in a truncation of the random variable,

$$\mathbf{X}^{k+1} = \widetilde{\mathbf{X}}^{k+1} \big| B(\alpha\sqrt{b}). \tag{2.16}$$

Here, for any random variable $\mathbf{Y}$ with distribution $p_{\mathbf{Y}}$ and a Borel set $C \subseteq \mathbb{R}^d$ with $p_{\mathbf{Y}}(C) > 0$, the random variable $\mathbf{Y}|C$ has *truncated distribution* $p_{\mathbf{Y}}(\,\cdot\,|C)$. In particular, if $\mathbf{Y}$ has density $f$, the random variable $\mathbf{Y}|C$ has density equal to $f/p_{\mathbf{Y}}(C)$ on $C$ and 0 otherwise.

# 3 Micro-macro acceleration method

Our micro-macro acceleration method aims at being faster than a full microscopic simulation, while converging to it when the extrapolation time step vanishes. The underlying assumption is that the macroscopic state variables can be simulated on a much slower timescale than the microscopic dynamics, thus allowing the choice of a large extrapolation time step compared with the time step for microscopic simulation. We introduce the restriction and matching operators (Section 3.1) to connect the two levels of description, then we discuss the extrapolation step (Section 3.2). We present specific matching operators in Section 4.

## 3.1 Matching and restriction operators

### 3.1.1 Moments of probability measures

Let $\mathscr{M}_1(G)$, where $G \subseteq \mathbb{R}^d$ is measurable, denote the set of all probability measures on $G$, i.e., all non-negative measures $\mu$ on $\mathbb{R}^d$ with support in G and such that $\mu(G) = 1$. For our analysis, we consider a sequence of moments $(m_l(\mu))_{l=1}^{\infty}$, obtained from $\mu$ by taking the expectations of given functions $R_l$, i.e.,

$$m_l(\mu) = \int_{\mathbb{R}^d} R_l(\mathbf{x})\, \mu(\mathrm{d}\mathbf{x}), \qquad l \geq 1. \tag{3.1}$$

Henceforward we will call $R_l$ the *moment function* and we will say that the value $m_l$ is the $l$-th moment of measure $\mu$.

The choice of the functions $R_l$ is problem-dependent. Clearly, they should be selected such that the integrals in (3.3) exist, at least for a subset of $\mathscr{M}_1(G)$ containing the laws of all trajectories of the SDE (1.1) in consideration. In our case it suffices that $R_l$ are in the class of continuous and polynomially bounded functions defined in Section 2.1.1. We also want each moment to hold new information about the measures, so that the functionals $\mu \mapsto m_l(\mu)$, $l \geq 1$ are linearly independent. Thus, we need an appropriate notion of independence for moment functions. Finally, we require a one-to-one correspondence between the measure $\mu$ and its full moment representation $(m_l(\mu))_{l=1}^{\infty}$. To collect all required properties, we introduce the following assumption (for more on the pseudo-Haar property, see [4] and Appendix A):

**Assumption 3.1.** *The functions $R_l$, $l \geq 1$, satisfy the following conditions:*
*a. they are linearly independent on every non-null subset of $G$ (pseudo-Haar);*
*b. for each $l$, $R_l \in C_P^0(\mathbb{R}^d, \mathbb{R})$ is non-constant;*
*c. if the law of the random variable $\mathbf{Z}$ is uniquely determined by all its moments, the same is true for $\mathbf{X}(s;t,\mathbf{Z})$, for any $0 \leq t < s \leq T$.*

*Example* 3.2. (Algebraic moments) In particular, we can consider $R_\alpha(\mathbf{x}) = \mathbf{x}^\alpha = x_1^{\alpha_1} \cdot \ldots \cdot x_d^{\alpha_d}$, $\mathbf{x} \in G$, where $\alpha \in \mathbb{N}_0^d$ is any multi-index, so that each value $m_\alpha(\mu)$ is the mixed raw moment of probability measure $\mu$. If $G = \mathbb{R}^d$ these moments exist for measures having densities decaying at infinity faster than any polynomial, and for all elements of $\mathscr{M}_1(G)$ if $G$ is bounded. The uniqueness of the moment representation is guaranteed by the existence of the moment generating function. In particular, Assumption 3.1 is satisfied if we consider FENE SDE (2.12) together with algebraic moments. ■

### 3.1.2 Definition and basic properties of restriction and matching

**Restriction.** To reduce the distributions to a finite collection of $L$ macroscopic state variables, we introduce a *restriction* operator

$$\mathcal{R}_L : \mathscr{M}_1(G) \to \mathbb{R}^L, \quad \mu \mapsto \mathcal{R}_L\mu. \tag{3.2}$$

The values of $\mathcal{R}_L$ represent the coarse-grained description of a microscopic law. We want to analyze the convergence of micro-macro acceleration method with increasing $L$, thus we will consider the hierarchy of restriction operators in which

$$\mathcal{R}_L\mu = \big(m_1(\mu), \dots, m_L(\mu)\big), \qquad L \geq 1, \tag{3.3}$$

i.e., we truncate the moment representation (3.1) of the measure $\mu$ to its first $L$ terms. Note that if one is only interested in approximating dynamics up to some tolerance, one may clearly consider the restriction operator in terms of a limited number of macroscopic state variables of interest, leaving the rest of the hierarchy unspecified.

**Matching.** Conversely, to obtain a probability measure (a law of a random variable) that is consistent with a finite set of $L$ macroscopic state variables, we consider a *matching* operator $\mathcal{P}_L$. Since we have to deal with distributions that are in general not uniquely determined by a finite set of macroscopic state variables, the matching represents the inference procedure with which we associate a law to this macroscopic state. This is the case for the laws arising in the FENE dumbbell model.

The idea of the matching operator is to use a *prior* measure $\mu \in \mathscr{M}_1(G)$ that we alter to make it consistent with the vector of (extrapolated) macroscopic states $\mathbf{m} \in \mathbb{R}^L$. In general, this is an underdetermined problem – infinitely many solutions are possible. One therefore has to choose a particular strategy that, at least under certain assumptions, will pick a unique distribution. In Section 4, we analyze a strategy based on a generalization of the *entropy principle*, which selects the consistent probability measure that is "closest" to the prior. Hence, the matching operator with $L$ moments will be defined, at least formally, as

$$\mathcal{P}_L(\mathbf{m}, \mu) = \operatorname*{argmin}_{\nu \in \mathcal{R}_L^{-1}(\mathbf{m})} d(\mu, \nu), \tag{3.4}$$

where $d(\cdot, \cdot)$ quantifies the (quasi-)distance between probability measures. We will consider $d$ to be an $L^2$-norm distance or an $f$-divergence [8].

*Remark* 3.3. We defined the restriction and matching operators as acting on probability measures. However, with a slight abuse of notation, we will also write $\mathcal{R}_L(\mathbf{X})$ and $\mathcal{P}_L(\mathbf{m}, \mathbf{X})$ for a random variable $\mathbf{X}$, meaning we consider its distribution as the argument in the operators. As a value of matching we take any random variable with the law given by $\mathcal{P}_L(\mathbf{m}, \mathbf{X})$. ■

**Restriction-matching pair.** The matching and restriction operators are related and need to be studied simultaneously. Thus, we introduce the following notion:

**Definition 3.4** (Restriction-matching pair)**.** Let $L \in \mathbb{N}$ and $G \subseteq \mathbb{R}^d$ be measurable. Assume that operators $\mathcal{R}_L \colon \mathscr{M}_1(G) \to \mathbb{R}^L$ and $\mathcal{P}_L \colon \mathbb{R}^L \times \mathscr{M}_1(G) \supseteq \operatorname{dom} \mathcal{P}_L \to \mathscr{M}_1(G)$, satisfy

1. $\mathcal{R}_L\left(\mathcal{P}_L(\mathbf{m}, \mu)\right) = \mathbf{m}$ for all $(\mathbf{m}, \mu) \in \operatorname{dom} \mathcal{P}_L$,
2. $\mathcal{P}_L(\mathcal{R}_L(\mu), \mu) = \mu$ for all $(\mathcal{R}_L(\mu), \mu) \in \operatorname{dom} \mathcal{P}_L$ (projection property).

Then we call $(\mathcal{R}_L, \mathcal{P}_L)$ the *restriction-matching pair* with $L$ macroscopic state variables.

A few remarks on the restriction-matching pair are in order.

*Remark* 3.5 (Domain of the matching operator). The first assumption in Definition 3.4 implies that $\operatorname{dom} \mathcal{P}_L \subseteq \operatorname{Im}\mathcal{R}_L \times \mathscr{M}_1(G)$, meaning that the moment vector $\mathbf{m}$ we consider must always correspond to at least one probability distribution. This is, of course, a necessary condition for the existence of the matched measure but it may not be sufficient, as we point

out in the case of matching based on $f$-divergences. In Section 6.3.1, we discuss the effect on the numerical behavior of trying to match a prior $\mu$ with a set of moments that are not realizable. We also restrict the domain to a subset of $\mathscr{M}_1(G)$, since sometimes not all measures can be obtained through the matching operator, for instance, if higher integrability or absolute continuity is required (see Section 4). ■

*Remark* 3.6 (The term projection). Let $\mathbf{m} \in \operatorname{im} \mathcal{R}_L$ and consider the mapping $\mathcal{P}_L(\mathbf{m}, \cdot)$. The second condition in Definition 3.4 implies that $\mathcal{P}_L^2(\mathbf{m}, \cdot) = \mathcal{P}_L(\mathbf{m}, \cdot)$. This justifies the use of the term projection. ■

We are now ready to formulate the main requirements on the sequences of restriction-matching pairs that allow us to show convergence of the micro-macro acceleration method to the full microscopic dynamics.

**Property 3.7** (Continuity of matching)**.** Fix $L \in \mathbb{N}$ and let $(\mathcal{R}_L, \mathcal{P}_L)$ be a restriction-matching pair with $L$ macroscopic state variables. We say that $\mathcal{P}_L$ is *(weakly) continuous* if for all $g \in C_P^0(G, \mathbb{R})$ there exists a constant $C_L = C_L(g) > 0$ such, that

$$\left|\mathbb{E}g(\mathcal{P}_L(\mathbf{m}^1, \mathbf{Z})) - \mathbb{E}g(\mathcal{P}_L(\mathbf{m}^2, \mathbf{Z}))\right| \leq C_L \|\mathbf{m}^1 - \mathbf{m}^2\|, \tag{3.5}$$

for every random variable $\mathbf{Z}$ and all vectors $\mathbf{m}^i \in \operatorname{Im}\mathcal{R}_L$ with $(\mathbf{m}^i, \mathbf{Z}) \in \operatorname{dom} \mathcal{P}_L$, $i = 1, 2$.

**Property 3.8** (Consistency of matching)**.** Consider a sequence of restriction-matching pairs $\{(\mathcal{R}_L, \mathcal{P}_L)\}_{L=1}^{\infty}$ with $\mathcal{R}_L$ given by (3.3) and satisfying Assumption 3.1. We say that this sequence is *consistent with equation* (1.1) if for any solution $\mathbf{X}$:

a. for all $L$ and $0 \leq t' \leq t \in I$ we have $\big(\mathcal{R}_L \mathbf{X}(t), \mathbf{X}(t')\big) \in \operatorname{dom} \mathcal{P}_L$;

b. for every $g \in C_P^{2(p+1)}(G, \mathbb{R})$ and $L \in \mathbb{N}$, there exists a constant $C_L = C_L(g) > 0$ such that

$$\left|\mathbb{E}g\big(\mathcal{P}_L(\mathbf{m}_L, \mathbf{Z})\big) - \mathbb{E}g\big(\mathbf{X}(t; t', \mathbf{Z})\big)\right| \leq C_L(t - t'), \tag{3.6}$$

for all $0 \leq t' \leq t \in I$ and all initial random variables $\mathbf{Z}$, where $\mathbf{m}_L = \mathcal{R}_L \mathbf{X}(t; t', \mathbf{Z})$;

c. for fixed $g \in C_P^{2(p+1)}(G, \mathbb{R})$, $C_L \to 0$ as $L \to +\infty$.

We study specific matching operators, and discuss Properties 3.7 and 3.8, in Section 4.

## 3.2 Extrapolation operator

In this manuscript we only consider first order extrapolation, which is reminiscent of forward Euler integration of the macroscopic state variables. This idea was first proposed in [21], see also [37, 38, 69].

We introduce two indices, $k = 0, \ldots, K$ and $n = 0, \ldots, N$, to emphasize the fact that there are two time steps involved: the microscopic time step $\delta t > 0$, over which we will evolve the full microscopic dynamics; and the macroscopic time step $\Delta t > 0$, over which we will perform extrapolation of the macroscopic state variables. The idea is to take a small number $K$ of microscopic steps of size $\delta t$, such that $K\delta t \ll \Delta t$, and from a microscopic simulation, starting at time $t^n = n\Delta t$, evaluate $\mathbf{m}^{n,k}$ at time $t^{n,k} = t^n + k\delta t$, for $k = 1, \ldots, K$, using the restriction operator (3.2). We then extrapolate as follows:

$$\mathbf{m}^{n+1} = \mathcal{E}\left((\mathbf{m}^{n,k})_{k=0}^K; \delta t, \Delta t\right) = \mathbf{m}^{n,0} + \frac{\Delta t}{K\delta t}(\mathbf{m}^{n,K} - \mathbf{m}^{n,0}), \tag{3.7}$$

in which $\mathbf{m}^{n,0} \equiv \mathbf{m}^n$. Clearly, the forward Euler extrapolation (3.7) satisfies:

$$\begin{aligned}\|\mathbf{m}_1^{n+1} - \mathbf{m}_2^{n+1}\| \leq \frac{\Delta t}{K\delta t}\|\mathbf{m}_1^{n,K} - \mathbf{m}_2^{n,K}\| + \Big(\frac{\Delta t}{K\delta t} - 1\Big)\|\mathbf{m}_1^{n,0} - \mathbf{m}_2^{n,0}\| \leq \\ \leq \frac{\Delta t}{K\delta t}\big(\|\mathbf{m}_1^{n,K} - \mathbf{m}_2^{n,K}\| + \|\mathbf{m}_1^{n,0} - \mathbf{m}_2^{n,0}\|\big),\end{aligned} \tag{3.8}$$

with any two sequences $\{\mathbf{m}_i^{n,k}\}_{k=0,\ldots,K}$, $i = 1, 2$, where in the first estimate we used the fact that $K\delta t \leq \Delta t$. Moreover, we have the following Lemma (the proof follows from a simple first-order Taylor expansion):

**Lemma 3.9** (Consistency of extrapolation)**.** *Let* $\widetilde{\mathbf{m}} \in C^2([t^n, t^{n+1}])$ *and put*

$$\mathbf{m}^{n+1} = \mathcal{E}\left((\widetilde{\mathbf{m}}(t^{n,k}))_{k=0}^K; \delta t, \Delta t\right)$$

*with the extrapolation operator* $\mathcal{E}$ *defined in* (3.7)*. Then, we have*

$$\|\widetilde{\mathbf{m}}(t^{n+1}) - \mathbf{m}^{n+1}\| \leq \max_{[t^n, t^{n+1}]} \|\widetilde{\mathbf{m}}''\| \cdot (\Delta t)^2.$$

Higher order versions of (3.7) can be constructed in several ways, e.g. using the polynomial extrapolation [21]. Adams-Bashforth or Runge-Kutta implementations of (3.7) are also possible [42, 43, 46, 55], as are implicit versions, partially discussed in [20]. Another idea, based on [64], trades accuracy for stability by designing a multistep state extrapolation method based on macroscopic states at multiple macroscopic time steps [68].

## 3.3 Description of the method and convergence result

Now that we have introduced all building blocks, we describe the method as a whole.

**Algorithm 3.10** (Micro-macro acceleration step)**.** Given a microscopic state $\mathbf{X}^n$ at time $t^n$, macroscopic step size $\Delta t > 0$, microscopic step size $\delta t > 0$, and a number $K \in \mathbb{N}$ of microscopic steps, with $K\delta t \leq \Delta t$, compute the microscopic state $\mathbf{X}^{n+1}$ at time $t^{n+1} = t^n + \Delta t$ via a four-step procedure:

1. *Simulate* the microscopic system over $K$ time steps of size $\delta t$ using a microscopic discretization scheme

$$\mathbf{X}^{n,k+1} = S^{n,k}(\mathbf{X}^{n,k}; \delta t), \quad k = 0, \ldots, K-1, \tag{3.9}$$

   defined in (2.4), with $\mathbf{X}^{n,0} = \mathbf{X}^n$.
2. *Record* the macroscopic states $\mathbf{m}^{n,k} = \mathcal{R}_L \mathbf{X}^{n,k}$ for $k = 0, \ldots, K$ using the restriction operator (3.2).
3. *Extrapolate* the macroscopic states $\mathbf{m}^{n,0}, \ldots, \mathbf{m}^{n,K}$ over a step of size $\Delta t$ to a new macroscopic state $\mathbf{m}^{n+1}$ at time $t^{n+1}$ using the extrapolation operator (3.7),

$$\mathbf{m}^{n+1} = \mathcal{E}\left((\mathbf{m}^{n,k})_{k=0}^K; \delta t, \Delta t\right). \tag{3.10}$$

4. *Match* the microscopic state $\mathbf{X}^{n,K}$ at time $t^{n,K}$ with the extrapolated macroscopic state $\mathbf{m}^{n+1}$ using the matching operator (3.4),

$$\mathbf{X}^{n+1} = \mathcal{P}_L(\mathbf{m}^{n+1}, \mathbf{X}^{n,K}), \tag{3.11}$$

   to obtain a new microscopic state $\mathbf{X}^{n+1}$ at time $t^{n+1}$.

*Remark* 3.11 (Numerical implementation). In the numerical implementation, we will need to consider a version of the algorithm that deals with an ensemble of realisations $\mathscr{X} = \{\mathbf{X}_j\}_{j=1}^J$ instead of the random variable $\mathbf{X}$. This will be discussed in Section 6. ■

Convergence of this method is guaranteed by the following theorem:

**Theorem 3.12.** *Consider the SDE* (1.1) *satisfying Assumption 2.1 and its solution* $\mathbf{X}$ *with initial condition* $\mathbf{X}(0) = \mathbf{X}^0$*. Let* $R_l \in C^4(G, \mathbb{R})$*,* $l \geq 1$*, be a sequence of moment functions, fulfilling Assumption 3.1, that generate restriction operators* $\mathcal{R}_L$*,* $L \geq 1$*, by* (3.3) *and let* $\{(\mathcal{R}_L, \mathcal{P}_L)\}_{L=1}^\infty$ *be a sequence of restriction-matching pairs having Properties 3.7 and 3.8. Furthermore, consider a time discretization scheme* (2.4) *of order* $p_S \geq 1$ *with time step* $\delta t$ *and satisfying Assumption 2.4. Finally, let* $\mathcal{E}$ *be the extrapolation operator* (3.7) *with extrapolation step* $\Delta t$ *and let* $K \in \mathbb{N}$ *be a number of microscopic steps with* $K\delta t \leq \Delta t$*.*

*If we denote the solution of Algorithm 3.10 with* $L$ *macroscopic state variables at time* $T$ *as* $\mathbf{X}_L^N$*, for any function* $g \in C_P^{2(p_S+1)}(G, \mathbb{R})$ *we have*

$$\left|\mathbb{E}\left[g(\mathbf{X}_L^N) - g(\mathbf{X}(T))\right]\right| \leq C_L + \widetilde{C}_L\left((\delta t)^{p_S} + \Delta t\right), \tag{3.12}$$

*in which* $C_L$ *and* $\widetilde{C}_L$ *are constants that depend also on* $T, g$ *and* $\mathbf{X}^0$*, with* $C_L \to 0$ *as* $L \to +\infty$*.*

The proof of Theorem 3.12 will be given in Section 5. Theorem 3.12 shows that the error of the micro-macro acceleration method is composed of three terms: (i) a matching error that depends only on the number $L$ of macroscopic state variables and that can be made arbitrarily small by choosing $L$ sufficiently large; (ii) a microscopic discretization error; and (iii) an extrapolation error. The last two errors can be made arbitrarily small by a suitable choice of $\delta t$ and $\Delta t$. Moreover, convergence does not rely on the precise definition of the restriction-matching pair, but only on its generic continuity and consistency properties. Specific restriction-matching pairs are discussed and analyzed in Section 4.

# 4 Matching operators

This Section is devoted to the investigation of specific matching operators that can be used in the micro-macro acceleration method. All operators are based on the minimization of a distance (Section 4.2) or an $f$-divergence (Section 4.3) between the probability density functions with the constraints given by the restriction operator.

## 4.1 Notations and function spaces

In this Section, we will work in the Lebesgue spaces $L^p(G,\mu)$ with norm $\|\cdot\|_p$, where $G \subset \mathbb{R}^d$ is open and bounded, $\mu$ is a finite Borel measure on $\mathbb{R}^d$ with full support on $G$ and $p \in [1,+\infty)$. We will also consider the convex set $\mathscr{P}^p(G) \subset L^p(G)$ of all probability densities integrable with $p$-th power, and the cone $L^p_+(G,\mu)$ of all non-negative functions in $L^p(G,\mu)$. Finally, recall that the dual space to $L^p(G,\mu)$ is isomorphic (congruent) to $L^q(G,\mu)$ with $q \in (1,+\infty]$ satisfying $1/p + 1/q = 1$ (see [30, p. 128]). The *dual pairing* between $\varphi \in L^q(G,\mu)$ and $\phi \in L^p(G,\mu)$ is given by

$$\langle \varphi,\, \phi \rangle = \int_G \varphi(\mathbf{x})\phi(\mathbf{x})\,\mu(\mathrm{d}\mathbf{x}).$$

Later on, we will specifically use $p = 1$ and $p = 2$.

By definition, for an appropriate vector $\mathbf{m} \in \mathbb{R}^L$ of moments and a prior density $\pi \in \mathscr{P}(G)$ the result of matching is a PDF, i.e., $\mathcal{P}_L(\mathbf{m},\pi) \in \mathscr{P}(G)$. Hence, we need to ensure that the solutions of minimization problem (3.4) integrate to one and are non-negative. We deal with the first requirement by adding the unity of the zeroth moment (mass) as an additional linear constraint. To avoid confusion with the constraints imposed by the moments $\mathbf{m}$, we introduce the (extended) restriction operator $\widetilde{\mathcal{R}}_L \colon L^p(G,\mu) \to \mathbb{R}^{L+1}$, in which, besides the finite number of moments, also the conservation of mass is included:

$$(\widetilde{\mathcal{R}}_L\phi)_l = \langle R_l,\, \phi \rangle \quad l = 0,\dots,L, \tag{4.1}$$

for some *moment functions* $R_l \in L^q(G,\mu)$, $l = 1,\dots,L$, and $R_0 \equiv 1 \in L^\infty(G,\mu)$, see also equation (3.3). The norm of this operator satisfies $|||\widetilde{\mathcal{R}}_L||| \le \|\mathbf{R}\|_q$, where $\mathbf{R} = (R_0,\dots,R_L)$ is the vector of moment functions. To ensure non-negativity of the solution we proceed in two ways. In Section 4.2, we do not include this property in the problem itself. Instead, we distinguish later the set of prior densities and moments for which positivity is preserved. This approach facilitates the analysis of the matching operator. In Section 4.3, we include this restriction directly in the minimization problem as a convex constraint using the cone $L^p_+(G)$. In this case all solutions are guaranteed to be PDFs, but the analysis becomes more difficult.

## 4.2 Matching with $L^2$ norm

First we construct a matching using the $L^2$ norm (L2N) $\|\cdot\|_2$ as a distance criterion between probability measures. Let $(R_l)_{l=1}^{+\infty} \subset L^2(G)$ be a sequence of non-constant, linearly independent moment functions. Fix $L \in \mathbb{N}$ and assume that we are given a prior PDF $\pi \in \mathscr{P}^2(G)$, uniquely determined by all its moments, and a vector of target moments $\mathbf{m} \in \mathbb{R}^L$ such, that $\mathbf{m} = \mathcal{R}_L(\Psi)$ for some density $\Psi \in \mathscr{P}^2(G)$.

Consider the optimal solution $\varphi_2(\mathbf{m}, \pi)$ to the problem

$$\begin{cases} \inf & \dfrac{1}{2}\|\varphi - \pi\|_2^2 \\ \text{s.t.} & \widetilde{\mathcal{R}}_L \varphi = (1, \mathbf{m}) \\ & \varphi \in L^2(G), \end{cases} \tag{4.2}$$

where $\widetilde{\mathcal{R}}_L$ is the restriction operator (4.1). Here we take $\mu$ to be the Lebesgue measure on $G$ and without loss of generality we can assume that the system $\{R_l\}_{l=0,1,\dots}$ is a basis for $L^2(G)$. The unique solution to problem (4.2) always exists, as can be seen by putting $\phi = \varphi - \Psi$ and considering equivalently the following least squares problem in $L^2(G)$:

$$\begin{cases} \inf & \dfrac{1}{2}\|\phi - (\pi - \Psi)\|_2^2 \\ \text{s.t.} & \phi \in \widetilde{\mathcal{R}}_L^{-1}(0), \end{cases} \tag{4.3}$$

in which the constraints imply that $\widetilde{\mathcal{R}}_L(\varphi) = \widetilde{\mathcal{R}}_L(\Psi)$. If we denote by $\{Q_l\}_{l=0,1,\dots}$ the orthonormal basis obtained from $\{R_l\}_{l=0,1,\dots}$ by the Gram-Schmidt orthogonalization procedure, we have $\widetilde{\mathcal{R}}_L^{-1}(0) = \overline{\operatorname{span}}\{Q_l : \ l \geq L+1\}$. This equality is an easy consequence of the fact that the change of basis in Gram-Schmidt orhonormalization procedure is described by the infinite lower triangular matrix $\widehat{Q}$ such, that

$$Q_l = \sum_{j=0}^{l} \widehat{Q}_{l,j} R_j, \quad l = 0, 1, \dots . \tag{4.4}$$

The solution to the least squares problem (4.3) is $\sum_{l=L+1}^{+\infty} \langle \pi - \Psi, Q_l \rangle \, Q_l$ (see, e.g., [3, Sec. 3.4 & 3.6]), so going back to $\varphi$ we obtain

$$\varphi_2(\mathbf{m}, \pi) = \sum_{l=0}^{L} \langle \Psi, Q_l \rangle \, Q_l + \sum_{l=L+1}^{+\infty} \langle \pi, Q_l \rangle \, Q_l. \tag{4.5}$$

Let us also mention that for fixed $\mathbf{m}$, $\varphi_2(\mathbf{m}, \cdot\,)$ is a non-expansive projection operator in $L^2(G)$ onto the hyperplane $\widetilde{\mathcal{R}}_L^{-1}(\mathbf{m})$ [3, Prop. 3.4.4]. Here non-expansiveness means $\|\varphi_2(\mathbf{m}, \pi_1) - \varphi_2(\mathbf{m}, \pi_2)\|_2 \leq \|\pi_1 - \pi_2\|_2$ for any $\pi_1, \pi_2 \in L^2(G)$.

To derive the formula in the original basis, let $\widehat{Q}_L$ be the $(L+1) \times (L+1)$ left upper submatrix of $\widehat{Q}$. Adding and subtracting $\pi$ on the right hand side of (4.5), and using the fact that for $l \leq L$ we can write $L$ in the upper limit of the sum in (4.4), we obtain

$$\begin{aligned} \varphi_2(\mathbf{m}, \pi) = \sum_{l=0}^{L} \langle \Psi - \pi, Q_l \rangle \, Q_l + \pi = \sum_{l=0}^{L} \sum_{i,j=0}^{L} \langle \Psi - \pi, R_j \rangle \, \widehat{Q}_{l,i} \widehat{Q}_{l,j} \, R_i + \pi = \\ = \sum_{i=0}^{L} \left( \sum_{j=0}^{L} (\widehat{Q}_L^T \widehat{Q}_L)_{i,j} \langle \Psi - \pi, R_j \rangle \right) R_i + \pi. \end{aligned}$$

Thus, if $H_L$ is the $(L+1) \times (L+1)$ matrix such, that $(H_L)^{-1} = \widehat{Q}_L^T \widehat{Q}_L$, we finally get

$$\varphi_2(\mathbf{m}, \pi) = \left[ H_L^{-1}(0, \mathbf{m} - \mathcal{R}_L \pi) \right]^T \mathbf{R} + \pi = \sum_{l=0}^{L} \lambda_l R_l + \pi, \tag{4.6}$$

where the coordinates of the vector $\left[ H_L^{-1}(0, \mathbf{m} - \mathcal{R}_L \pi) \right]^T$, denoted by $\lambda_l$, can be viewed as Lagrange multipliers. The entries of $H_L$ are of the form

$$(H_L)_{k,l} = \int_G R_k(\mathbf{x}) R_l(\mathbf{x}) \, \mathrm{d}\mathbf{x}, \tag{4.7}$$

for $k, l = 0, \dots, L$, as can be seen from (4.4) using the identity $\langle Q_k, Q_l \rangle = \delta_{k,l}$.

Of course, $\varphi_2(\mathbf{m}, \pi)$ has mass one but can in general be negative on the set of positive Lebesgue measures, thus it corresponds to a signed measure. However, we can ensure positivity when the prior distribution is bounded away from zero on $G$ and the target moments $\mathbf{m}$ are close enough to the moments of the prior $\pi$. The following Lemma is an easy consequence of representation (4.6).

**Lemma 4.1.** *Assume that $\pi \geq c$ a.e. on $G$ for some constant $c > 0$. There exists a constant $\delta = \delta(L, G, \mathbf{R}) > 0$ such that if $|\mathbf{m} - \mathcal{R}_L \pi| < \delta$, we have $\varphi_2(\mathbf{m}, \pi) \geq 0$ a.e. on $G$.*

*Remark* 4.2 (Matching for FENE dumbbells). The above results allow us to define, in particular, the $L^2$ matching operator for prior densities $\pi$ which correspond to the truncated random variables obtained in (2.15)-(2.16). In fact, let $\pi \in L^2(G)$ and for $\alpha \geq 0$ let us denote $G_\alpha = \{\mathbf{x} \in G : \ \|\mathbf{x} - \boldsymbol{\eta}\| > \alpha, \forall \boldsymbol{\eta} \in \partial G\}$. Assume that $\pi$ has support in $G_\alpha$ and that $\pi > c$ a.e. on $G_\alpha$ for some $c > 0$. Then, for every $\mathbf{m} \in \mathbb{R}^L$ close enough to $\mathcal{R}_L \pi$ we can define the matching operator as

$$\mathcal{P}_L(\mathbf{m}, \pi) = \begin{cases} \varphi_2(\mathbf{m}, \pi_{|G_\alpha}) & \text{on } G_\alpha, \\ 0 & \text{on } G \backslash G_\alpha. \end{cases} \tag{4.8}$$

■

Let us now analyze operator $\varphi_2$. The continuity of matching (Property 3.7) follows from:

**Lemma 4.3.** *Let $\pi, \Psi, \widetilde{\Psi} \in \mathscr{P}^2(G)$, and let $\mathbf{m}_L = \mathcal{R}_L \Psi$, $\widetilde{\mathbf{m}}_L = \mathcal{R}_L \widetilde{\Psi}$ with $L \in \mathbb{N}$. Then*

$$\|\varphi_2(\mathbf{m}_L, \pi) - \varphi_2(\widetilde{\mathbf{m}}_L, \pi)\|_2 \leq \|\widehat{Q}_L\| \cdot \|\mathbf{m}_L - \widetilde{\mathbf{m}}_L\|. \tag{4.9}$$

*Proof.* Let us denote by $\pi_l, \Psi_l, \widetilde{\Psi}_l$ the $l$-th Fourier coefficient of $\pi, \Psi, \widetilde{\Psi}$ respectively in the basis $\{Q_l\}_{l=0,1,\dots}$. Note that for $\varphi_2(\mathbf{m}_L, \pi)$ and $\varphi_2(\widetilde{\mathbf{m}}_L, \pi)$ only the first sum in expansion (4.5) differs. Thus, Parseval's identity implies

$$\|\varphi_2(\mathbf{m}_L, \pi) - \varphi_2(\widetilde{\mathbf{m}}_L, \pi)\|_2^2 = \left\| \sum_{l=0}^{L} (\Psi_l - \widetilde{\Psi}_l) Q_l \right\|_2^2 = \sum_{l=0}^{L} (\Psi_l - \widetilde{\Psi}_l)^2.$$

Now, according to (4.4), we have $(\Psi_0, \dots, \Psi_L) = \widehat{Q}_L \mathbf{m}_L$ and $(\widetilde{\Psi}_0, \dots, \widetilde{\Psi}_L) = \widehat{Q}_L \widetilde{\mathbf{m}}_L$. Hence, we finally obtain

$$\|\varphi_2(\mathbf{m}_L, \pi) - \varphi_2(\widetilde{\mathbf{m}}_L, \pi)\|_2^2 = \|\widehat{Q}_L(\mathbf{m}_L - \widetilde{\mathbf{m}}_L)\|^2,$$

from which (4.9) follows. □

To prove consistency (Property 3.8), we assume $G = (-\gamma, \gamma) \subset \mathbb{R}$ and that the moment functions are given as

$$R_l(x) = x^l, \quad l = 0, 1, \dots \ , \tag{4.10}$$

so that the restriction operator $\mathcal{R}_L$ extracts the first $L$ raw moments. For a given prior probability density $\pi \in L^2(-\gamma, \gamma)$ the solution to (4.2) is

$$\varphi_2(\mathbf{m}, \pi)(x) = \boldsymbol{\lambda}^T \mathbf{R}(x) + \pi(x) = \sum_{l=0}^{L} \lambda_l x^l + \pi(x), \tag{4.11}$$

where $\boldsymbol{\lambda} = H_L^{-1} \widetilde{\mathcal{R}}_L (\Psi - \pi)$ and according to (4.7)

$$H_{i,j} = \frac{1 + (-1)^{i+j}}{i + j + 1} \gamma^{i+j+1} \tag{4.12}$$

for $i, j = 0, \dots, L$. The set $\{R_l : \ l = 0, 1, \dots\} \subset L^\infty(-\gamma, \gamma)$ is the monomial basis of $L^2(-\gamma, \gamma)$ and its Gram-Schmidt orthonormalization $Q_l \in L^\infty(-\gamma, \gamma)$, $l = 0, 1, \dots$ , satisfies $Q_l(x) = P_l(x/\gamma)/\sqrt{\gamma}$ with $P_l$ the $l$-th (normalized) Legendre polynomial on $(-1, 1)$.

Before stating the main result of this section, Theorem 4.6, let us establish two supporting Lemmas.

**Lemma 4.4.** *Let $\phi \in C^2([-\gamma,\gamma])$ and let $\phi_l = \int_{-\gamma}^{\gamma} Q_l(x)\phi(x)\,\mathrm{d}x$, $l = 0,1,\dots$, denote its Fourier coefficients with respect to $\{Q_l\}$. Then*

$$\gamma \sum_{l=0}^{+\infty} l(l+1)|\phi_l|^2 = \int_{-\gamma}^{\gamma} \left(\gamma^2 - x^2\right) |\phi'(x)|^2 \,\mathrm{d}x. \tag{4.13}$$

The proof is a straightforward generalization of the proof in [65] that uses the relation between $Q_l$ and the Legendre polynomials. For the second Lemma let us denote by $W^{1,2}([-\gamma,\gamma])$ the Sobolev space of all functions $\phi \in L^2([-\gamma,\gamma])$ such that $\phi' \in L^2([-\gamma,\gamma])$ with norm $\|\phi\|_{1,2} = \|\phi\|_2 + \|\phi'\|_2$.

**Lemma 4.5.** *Fix $L \in \mathbb{N}$, $\Psi \in \mathscr{P}^2([-\gamma,\gamma])$ and let $\mathbf{m}_L = \mathcal{R}_L\Psi$. The projection operator $\varphi_2(\mathbf{m}_L,\cdot\,)$ is continuous in $W^{1,2}([-\gamma,\gamma])$.*

*Proof.* Let us take $(\phi_n)_{n=0}^{+\infty} \subset W^{1,2}([-\gamma,\gamma])$ such that $\lim_{n\to\infty} \|\phi_n - \phi_0\|_{1,2} = 0$. According to (4.11), $\varphi_2(\mathbf{m}_L,\phi_n)$ is the sum of $\phi_n$ and a polynomial, so it belongs to $W^{1,2}([-\gamma,\gamma])$ and we obtain

$$\begin{aligned}\|\varphi_2(\mathbf{m}_L,\phi_n)' - \varphi_2(\mathbf{m}_L,\phi_0)'\|_2 &\le \|\phi_n' - \phi_0'\|_2 + \left\| \sum_{l=0}^{L-1} (l+1)(\lambda_{l+1}^n - \lambda_{l+1}^0) R_l \right\|_2 \le \\ &\le \|\phi_n' - \phi_0'\|_2 + L \sum_{l=0}^{L-1} |\lambda_{l+1}^n - \lambda_{l+1}^0| \cdot \|R_l\|_2 \le \|\phi_n' - \phi_0'\|_2 + L\|\boldsymbol{\lambda}^n - \boldsymbol{\lambda}^0\| \cdot \|\mathbf{R}\|_2\end{aligned}$$

where $\boldsymbol{\lambda}^n = H_L^{-1}(0, \mathbf{m}_L - \mathcal{R}_L\phi_n)$ and the last estimate is based on the Hölder inequality. Moreover, using the estimate on the norm of $\widetilde{\mathcal{R}}_L$ we have

$$\|\boldsymbol{\lambda}^n - \boldsymbol{\lambda}^0\| \le \|H_L^{-1}\| \cdot \|\widetilde{\mathcal{R}}_L(\phi_n - \phi_0)\| \le \|H_L^{-1}\| \cdot \|\mathbf{R}\|_2 \cdot \|\phi_n - \phi_0\|_2$$

with $\|H_L^{-1}\|$ the matrix norm. Combining these two estimates and the non-expansiveness of $\varphi_2(\mathbf{m}_L,\cdot)$ gives

$$\|\varphi_2(\mathbf{m}_L,\phi_n) - \varphi_2(\mathbf{m}_L,\phi_0)\|_{1,2} \le \left(1 + L\|H_L^{-1}\| \cdot \|\mathbf{R}\|_2^2\right)\|\phi_n - \phi_0\|_2 + \|\phi_n' - \phi_0'\|_2,$$

from which the continuity follows. □

**Theorem 4.6.** *Let $L \in \mathbb{N}$ and let $\pi, \Psi \in W^{1,2}([-\gamma,\gamma])$ be two probability densities. If $\mathbf{m}_L = \mathcal{R}_L\Psi$ we have*

$$\|\varphi_2(\mathbf{m}_L,\pi) - \Psi\|_2 \le \frac{\sqrt{\gamma}}{(L+1)} \|\pi' - \Psi'\|_2. \tag{4.14}$$

*Proof.* First assume that $\pi, \Psi \in C^2([-\gamma,\gamma])$ and let $\pi_l, \Psi_l$ denote the $l$-th Fourier coefficients of $\pi$ and $\Psi$ respectively in the basis $\{Q_l\}_{l=0,1,\dots}$ (which is the orthonormalization of (4.10)). Then, using expansion (4.5) and Parseval's identity, we get

$$\begin{aligned}\|\varphi_2(\mathbf{m}_L,\pi) - \Psi\|_2^2 &= \sum_{l=L+1}^{+\infty} (\Psi_l - \pi_l)^2 \le \\ &\le \sum_{l=L+1}^{+\infty} \frac{l(l+1)}{(L+1)^2} (\Psi_l - \pi_l)^2 \le \frac{1}{(L+1)^2} \sum_{l=0}^{+\infty} l(l+1)(\Psi_l - \pi_l)^2.\end{aligned}$$

Finally, employing (4.13) from Lemma 4.4, we obtain

$$\|\varphi_2(\mathbf{m}_L,\pi) - \Psi\|_2^2 \le \frac{1}{\gamma(L+1)^2} \int_{-\gamma}^{\gamma} \left(\gamma^2 - x^2\right) |\Psi'(x) - \pi'(x)|^2 \,\mathrm{d}x \le \frac{\gamma}{(L+1)^2} \|\Psi' - \pi'\|_2^2.$$

Now let $\pi, \Psi \in W^{1,2}([-\gamma,\gamma])$ and take two sequences $(\pi_n)_n, (\Psi_n)_n \in C^2([-\gamma,\gamma])$ such that $\pi_n \to \pi$ and $\Psi_n \to \Psi$ in $W^{1,2}$. Then $\varphi_2(\mathbf{m}_L, \pi_n)$, $\varphi_2(\mathbf{m}_L, \Psi_n)$ are twice continuously differentiable for each $n$, and, according to Lemma 4.5, $\varphi_2(\mathbf{m}_L, \pi_n) \to \varphi_2(\mathbf{m}_L, \pi)$ and $\varphi_2(\mathbf{m}_L, \Psi_n) \to \varphi_2(\mathbf{m}_L, \Psi) = \Psi$ in $W^{1,2}$. Hence, using the first part of the proof together with $\mathbf{m}_L = \mathcal{R}_L\varphi_2(\mathbf{m}_L, \Psi_n)$, we get

$$\|\varphi_2(\mathbf{m}_L,\pi) - \Psi\|_2^2 = \lim_{n\to\infty} \|\varphi_2(\mathbf{m}_L,\pi_n) - \varphi_2(\mathbf{m}_L,\Psi_n)\|_2 \leq$$
$$\leq \frac{\sqrt{\gamma}}{(L+1)} \lim_{n\to\infty} \|\pi_n' - \varphi_2(\mathbf{m}_L,\Psi_n)'\|_2 = \frac{\sqrt{\gamma}}{(L+1)}\|\pi' - \Psi'\|_2,$$

which finishes the proof of (4.14). □

From Theorem 4.6 the following corollary follows that implies (3.6) from Property 3.8. Recall our convention for notation from Remark 3.3.

**Corollary 4.7.** *Let $X$ be a solution of (1.1) with a smooth density $\rho$. For every $t, t+\Delta t \in I$, with $\Delta t > 0$, put $\pi = \rho(t,\cdot)$, $\Psi = \rho(t+\Delta t,\cdot)$ and assume that $\varphi_2(\mathbf{m}_L,\pi) \geq 0$, where $\mathbf{m}_L = \mathcal{R}_L\Psi$. Then for every $g \in C([-\gamma,\gamma])$ we have*

$$\big|\mathbb{E}g\big(\varphi_2(\mathbf{m}_L, X(t))\big) - \mathbb{E}g\big(X(t+\Delta t)\big)\big| \leq \frac{C}{L+1}\Delta t, \tag{4.15}$$

*with $C$ depending only on $g$, $\rho$, $T$ and $\gamma$.*

*Proof.* Using formula (2.8) we obtain

$$\big|\mathbb{E}g\big(\varphi_2(\mathbf{m}_L, X(t)\big) - \mathbb{E}g\big(X(t+\Delta t)\big)\big| \leq \int_{-\gamma}^{\gamma} |g(y)||\varphi_2(\mathbf{m}_L,\pi) - \Psi| \,\mathrm{d}y$$
$$\leq 2\gamma \cdot \max_{[-\gamma,\gamma]} |g| \cdot \|\varphi_2(\mathbf{m}_L,\pi) - \Psi\|_2$$

According to Theorem 4.6, it is enough to estimate the $L^2$ norm between the derivatives of $\pi$ and $\Psi$. Applying the mean value theorem, we get

$$|\partial_x\rho(t+\Delta t,x) - \partial_x\rho(t,x)| \leq \max_{[0,T]\times[-\gamma,\gamma]} |\partial_t\partial_x\rho| \cdot \Delta t,$$

for every $x \in (-\gamma,\gamma)$. Hence

$$\|\Psi' - \pi'\|_2^2 = \int_{-\gamma}^{\gamma} |\partial_x\rho(t+\Delta t,x) - \partial_x\rho(t,x)|^2 \,\mathrm{d}x \leq 2\gamma \cdot \max_{[0,T]\times[-\gamma,\gamma]} |\partial_t\partial_x\rho|^2 \cdot (\Delta t)^2$$

Combining these estimates with Theorem 4.6 gives the result. □

We provide a sufficient condition for the existence and smoothness of $\rho$ in Section 2.2.1 for the specific example of FENE dumbbells.

## 4.3 Matching with $f$-divergences

Let $p \in [1,+\infty)$ and let $\mathcal{R}_L\colon \mathscr{P}^p(G) \to \mathbb{R}^L$ be the restriction operator (3.3) generated by the functions $R_1,\dots,R_l \in L^p(G)$. In this section, we consider matching operators that for a vector of macroscopic state variables $\mathbf{m} \in \mathrm{Im}\mathcal{R}_L$ and a prior distribution $\pi \in \mathscr{P}^p(G)$ are defined as

$$\mathcal{P}_L(\mathbf{m},\pi) = \operatorname*{argmin}_{\varphi\in\mathcal{R}_L^{-1}(\mathbf{m})} \mathcal{I}_f(\varphi\,|\pi), \tag{4.16}$$

where $\mathcal{I}_f(\,\cdot\,|\pi)$ is a *divergence functional* generated by a function $f\colon [0,+\infty) \to [0,+\infty)$

$$\mathcal{I}_f(\varphi|\pi) = \begin{cases} \displaystyle\int_G f\left(\frac{\varphi(\mathbf{x})}{\pi(\mathbf{x})}\right)\pi(\mathbf{x})\,\mathrm{d}\mathbf{x} & \text{if } \operatorname{supp}\varphi \subseteq \operatorname{supp}\pi, \\ +\infty & \text{otherwise,} \end{cases} \qquad \varphi \in \mathscr{P}^p(G). \tag{4.17}$$

Note that the condition $\operatorname{supp}\varphi \subseteq \operatorname{supp}\pi$ is equivalent to requiring that the measure $\mu_\varphi$ corresponding to the density $\varphi$ is absolutely continuous with respect to the measure $\mu_\pi$ corresponding to $\pi$, which we denote as $\mu_\varphi \ll \mu_\pi$.

We assume that $f$ is not identically equal to zero, lower semi-continuous, convex and such that $f(1) = 0$. Let us denote by $f_+$ the extension of $f$ to the whole real line such that $f_+(t) = +\infty$ for negative $t$. If we consider the probability measure $\mu_\pi$ (generated by $\pi$) and put $\phi = \varphi/\pi \in L^p(G, \mu_\pi)$ for each $\varphi \in \mathscr{P}^p(G)$ such that $\mu_\varphi \ll \mu_\pi$, we see that (4.16) is equivalent to the *primal (entropy) problem* $(EP)_p$ in $L^p(G, \mu_\pi)$, see Appendix A, with vector $\widetilde{\mathbf{m}} = (1, \mathbf{m}) \in \mathbb{R}^{L+1}$. Recall that in $(EP)_p$ we ensure that the optimal solution, if it exists, is a probability density by using the extended restriction operator $\widetilde{\mathcal{R}}_L$, with additional moment function $R_0 \equiv 1$, and a convex constraint to the cone $L^p_+(G, \mu_\pi)$.

If all assumptions of Theorem A.1 are satisfied, it follows from (A.4) that the explicit formula for the matching operator defined by (4.16) is given by

$$\mathcal{P}_L(\mathbf{m}, \pi) = (f_+^*)'\left(\sum_{l=0}^{L} \overline{\lambda}_l R_l\right) \cdot \pi, \tag{4.18}$$

where $(f_+^*)'$ is the derivative of the convex conjugate $f_+^*$ (defined in (A.1)) and the multipliers $\overline{\lambda}_0, \ldots, \overline{\lambda}_L$ satisfy the Lagrangian dual problem (cf. (A.5))

$$\widetilde{\mathbf{m}} - \widetilde{\mathcal{R}}_L\left((f_+^*)'\Big(\sum_{l=0}^{L} \overline{\lambda}_l R_l\Big)\right) = 0. \tag{4.19}$$

The derivation of this dual problem is presented in Appendix A. The general result on the existence of solution is given as Theorem A.1, which is a specialization of a result from [4] to our setting. In particular, note that condition (A.3) requires additionally the vector $\mathbf{m}$ to lie in the interior of the image of $\mathcal{R}_L$ (cf. Remark 3.5)

We now consider two specific examples: the Kullback-Leibler divergence and the $L^2$-divergence. While we do not show rigorously that Property 3.8 holds for these matching operators at this point, we will illustrate in Section 6 that the numerical behaviour of these matchings is very similar to that of the $L^2$-norm matching of Section 4.2, while offering two significant advantages. First, $f$-divergence matching guarantees positivity of the resulting matched probability density. Second, $f$-divergence matching leads to numerical methods that are easier to implement numerically for ensembles of finite size.

**Kullback-Leibler divergence.** Here, we take as generating function

$$f(t) = \begin{cases} t \ln t - t + 1 & t > 0, \\ 1 & t = 0, \end{cases} \tag{4.20}$$

and consider the resulting divergence distance on $\mathscr{P}(G)$ (thus $p = 1$ in this case). With this choice of $f$ the resulting functional is (the term generated by $-t + 1$ cancels out)

$$\mathcal{I}_f(\varphi|\pi) = \int_G \frac{\varphi(\mathbf{x})}{\pi(\mathbf{x})} \ln\left(\frac{\varphi(\mathbf{x})}{\pi(\mathbf{x})}\right) \pi(\mathbf{x})\,\mathrm{d}\mathbf{x}, \quad \mu_\varphi \ll \mu_\pi,$$

which is called Kullback-Leibler divergence (KLD) or logarithmic relative entropy. The dual of $f_+$ is $f_+^*(s) = \exp(s) - 1$, $s \in \mathbb{R}$. Note that $f$ satisfies the assumptions in Theorem A.1. Hence, if the moment functions $R_1, \ldots, R_l$ fulfill Assumption 3.1(a) and (A.3) holds, the formula for matching (4.18) reads

$$\mathcal{P}_L(\mathbf{m}, \pi) = \exp\left(\sum_{l=0}^{L} \overline{\lambda}_l R_l\right) \cdot \pi, \tag{4.21}$$

with $\overline{\lambda}_0, \ldots, \overline{\lambda}_L$ the solution to the non-linear system of integral equations (recall $R_0 \equiv 1$)

$$\begin{cases} e^{\lambda_0} \int_G R_l \exp\left(\sum_{k=1}^{L} \lambda_k R_k\right) \pi \, \mathrm{d}\mathbf{x} = m_l, \quad l = 1, \ldots, L, \\ \lambda_0 = -\ln \int_G \exp\left(\sum_{k=1}^{L} \lambda_k R_k\right) \pi \, \mathrm{d}\mathbf{x}. \end{cases} \tag{4.22}$$

It is not possible to analytically solve (4.22), so we will use a Newton-Raphson procedure to perform the optimization numerically, see Appendix B.

*Remark* 4.8. (Reducing dimensions for KLD based matching) To keep the mass of the matching equal to 1 we include the additional linear constraint with moment function $R_0$ and obtain 0-th Lagrange multiplier $\lambda_0$ in the dual problem. This implies that we perform the optimization in $L+1$ dimensions and that the resulting numerical solution has mass one only up to the tolerance of the Newton-Raphson procedure. With KLD based matching we can express $\lambda_0$ as a function of the other multipliers, see (4.22), thus reducing the dimensionality by one and keeping the mass of the numerical solution (and in fact solutions corresponding to all steps of Newton-Raphson iteration) equal to one up to the machine precision. However, in this case we observed that the convergence of the Newton-Raphson procedure is slower compared to $L+1$ dimensional optimization, so we decided not to use this approach. ■

**$L^2$ divergence** Our second example is based on the generating function

$$f(t) = \frac{1}{2}(t-1)^2, \quad t \geq 0. \tag{4.23}$$

Hence, if $\varphi, \pi \in \mathscr{P}^2(G)$ and $\mu_\varphi \ll \mu_\pi$, the divergence distance under consideration is

$$\mathcal{I}_f(\varphi \,|\pi) = \frac{1}{2} \int_G \left(\frac{\varphi(\mathbf{x})}{\pi(\mathbf{x})} - 1\right)^2 \pi(\mathbf{x}) \, \mathrm{d}\mathbf{x},$$

which is called $L^2$ divergence (L2D) or quadratic relative entropy. The dual of $f_+$ in this case is $f_+^*(s) = 1/2\,[\max(0, s+1)^2 - 1]$. Since $f$ satisfies the assumptions in Theorem A.1, under Assumption 3.1(a) and (A.3), the formula for matching (4.18) reads

$$\mathcal{P}_L(\mathbf{m}, \pi) = \max\left(0, \sum_{l=0}^{L} \overline{\lambda}_l R_l\right) \cdot \pi, \tag{4.24}$$

where $\overline{\lambda}_0, \ldots, \overline{\lambda}_L$ solve

$$m_l - \int_G R_l(\mathbf{x}) \max\left(0, \sum_{k=0}^{L} \lambda_k R_k(\mathbf{x})\right) \pi(\mathbf{x}) \, \mathrm{d}\mathbf{x} = 0, \quad l = 0, \ldots, L. \tag{4.25}$$

We again need to find the solution to (4.25) numerically; see Appendix B for the corresponding Newton-Raphson procedure.

# 5 Proof of the convergence result

Throughout this Section we use the notation of Section 3.3 and suppose that all the assumptions of Theorem 3.12 hold. The proof requires the following Lemmas:

**Lemma 5.1.** *For every sufficiently large $r$ there is a constant $C_{L,r,T} > 0$ such that*

$$\mathbb{E}\|\mathbf{X}^n\|^{2r} \leq C_{L,r,T}(1 + \|\mathbf{X}^0\|^{2r})$$

*for all $N, K$ and $n = 1, \ldots, N$, $k = 1, \ldots, K$.*

*Proof.* Fix $n < N$. According to the uniform boundedness of the moments for the one-step microscopic discretization $S$ (Assumption 2.4), for every sufficiently large $r > 0$ there is a constant $C_{r,T} > 0$ such that $\mathbb{E}\|X^{n,k}\|^{2r} \le C_{r,T}\mathbb{E}\|X^{n,0}\|^{2r}$ for all $k = 1, \dots, K$. Let us also take constants $\widehat{C}_{l,T}$, $\widehat{\kappa}_{l,T}$ from Lemma 2.5 and $\widetilde{C}_{l,T}$, $\widetilde{\kappa}_{l,T}$ from estimate (2.2), corresponding to the functions $R_l$, $l = 1, \dots, L$. For each $r$ sufficiently large it holds with $C_{L,r,T} = 2(\widehat{C}_{l,T} + \widetilde{C}_{l,T})$

$$\widehat{C}_{l,T}(1 + \|\mathbf{z}\|^{2\widehat{\kappa}_{l,T}}) + \widetilde{C}_{l,T}(1 + \|\mathbf{z}\|^{2\widetilde{\kappa}_{l,T}}) \le C_{L,r,T}(1 + \|\mathbf{z}\|^{2r})$$

for all $\mathbf{z} \in G$ and $l = 1, \dots, L$.

Let us now fix $r$ large enough so that the discussion in the previous paragraph applies. For every $l \le L$, using Lemma 2.5 and formula (2.2), we have

$$\begin{aligned}\left|\mathbb{E}R_l(\mathbf{X}^{n,K}) - \mathbb{E}R_l(\mathbf{X}^{n,0})\right| &\le \left|\mathbb{E}R_l(\mathbf{X}^{n,K}) - \mathbb{E}R_l(\mathbf{X}(t^{n,K}; t^{n,0}, \mathbf{X}^{n,0}))\right| + \\ + \left|\mathbb{E}R_l(\mathbf{X}(t^{n,K}; t^{n,0}, \mathbf{X}^{n,0})) - \mathbb{E}R_l(\mathbf{X}^{n,0})\right| &\le \widehat{C}_{l,T}(1 + \mathbb{E}\|\mathbf{X}^{n,0}\|^{2\widehat{\kappa}_{l,T}})K(\delta t)^{p+1} + \\ + \widetilde{C}_{l,T}(1 + \mathbb{E}\|\mathbf{X}^{n,0}\|^{2\widetilde{\kappa}_{l,T}})K\delta t &\le C_{L,r,T}(1 + \mathbb{E}\|\mathbf{X}^{n,0}\|^{2r})K\delta t, \quad (5.1)\end{aligned}$$

where we estimated $(\delta t)^p \le T^p$ and absorbed the factor $T^p$ into the constant $C_{L,r,T}$.

Recall that $\mathbf{X}^{n+1} = \mathcal{P}_L(\mathbf{m}^{n+1}, \mathbf{X}^{n,K})$, from the definition, and $\mathbf{X}^{n,K} = \mathcal{P}_L(\mathbf{m}^{n,K}, \mathbf{X}^{n,K})$, from the properties of matching. Thus employing the continuity of matching (Property 3.7) and formula (3.7) (for the extrapolation) we obtain

$$\begin{aligned}\mathbb{E}\|\mathbf{X}^{n+1}\|^{2r} \le \left|\mathbb{E}\|\mathbf{X}^{n+1}\|^{2r} - \mathbb{E}\|\mathbf{X}^{n,K}\|^{2r}\right| + \mathbb{E}\|\mathbf{X}^{n,K}\|^{2r} &\le C_{L,r}\left\|\mathbf{m}^{n+1} - \mathbf{m}^{n,K}\right\| + \\ + C_{r,T}\mathbb{E}\|\mathbf{X}^{n,0}\|^{2r} &\le C_{L,r}\frac{\Delta t}{K\delta t}\left\|\mathbf{m}^{n,K} - \mathbf{m}^{n,0}\right\| + C_{r,T}\mathbb{E}\|\mathbf{X}^{n}\|^{2r}.\end{aligned}$$

Since $\|\mathbf{m}^{n,K} - \mathbf{m}^{n,0}\| \le L \cdot \max_{l \le L} |\mathbb{E}R_l(\mathbf{X}^{n,K}) - \mathbb{E}R_l(\mathbf{X}^{n,0})|$, from (5.1) we get

$$\mathbb{E}\|\mathbf{X}^{n+1}\|^{2r} \le L\, C_{L,r}C_{L,r,T}\Delta t(1 + \mathbb{E}\|\mathbf{X}^{n}\|^{2r}) + C_{r,T}\mathbb{E}\|\mathbf{X}^{n}\|^{2r}.$$

This recurrence implies by [51, Lem. 1.3.] that $\mathbb{E}\|\mathbf{X}^{n+1}\|^{2r} \le e^C(1 + \mathbb{E}\|\mathbf{X}^0\|^{2r})$ for a constant $C$ depending only on $r$, $L$ and $T$. □

**Lemma 5.2.** *There is a constant $C^{\mathcal{E}}_{L,T}$ such that for all $N$, $K$ and $n = 0, \dots, N$, $k = 0 \dots, K$*

$$\|\mathcal{E}\big((\mathcal{R}_L\mathbf{X}(t^{n,k}; t^n, \mathbf{X}^n))_{k=0}^K; \Delta t, \delta t\big) - \mathcal{R}_L\mathbf{X}(t^{n+1}; t^n, \mathbf{X}^n)\| \le C^{\mathcal{E}}_{L,T} \cdot (\Delta t)^2.$$

*Proof.* Put $\widetilde{\mathbf{m}}^n(s) = \mathcal{R}_L\mathbf{X}(s; t^n, \mathbf{X}^n)$, $s \in [t^n, t^{n+1}]$. Assumption 2.1.a together with the fact that $R_l \in C^4_P(G, \mathbb{R})$ imply: $\widetilde{\mathbf{m}}^n \in C^2([t^n, t^{n+1}], \mathbb{R})$. Thus from Lemma 3.9 we obtain

$$\|\mathcal{E}\big((\mathcal{R}_L\mathbf{X}(t^{n,k}; t^n, \mathbf{X}^n))_{k=0}^K; \Delta t, \delta t\big) - \mathcal{R}_L\mathbf{X}(t^{n+1}; t^n, \mathbf{X}^n)\| \le \max_{s \in [t^n, t^{n+1}]} \|(\widetilde{\mathbf{m}}^n)''(s)\| \cdot (\Delta t)^2$$

and from Lemma 5.1 we can find $\kappa_{L,T}$ and $C_{L,T}$ large enough such that

$$\begin{aligned}\max_{s \in [t^n, t^{n+1}]} \|(\widetilde{\mathbf{m}}^n)''(s)\| \le L \cdot \max_{s \in [t^n, t^{n+1}]} \max_{l \le L} \left|\partial_s^2\, \mathbb{E}R_l\big(\mathbf{X}(s; t^n, \mathbf{X}^n)\big)\right| &\le \\ \le L \cdot \max_{l \le L} \widetilde{C}_{l,T}\big(1 + \mathbb{E}\|\mathbf{X}^n\|^{2\widetilde{\kappa}_{l,T}}\big)^2 &\le C_{L,T}(1 + \mathbb{E}\|\mathbf{X}^0\|^{2\kappa_{L,T}})^2,\end{aligned}$$

where $\widetilde{C}_{l,T}$, $\widetilde{\kappa}_{l,T}$ are constants from Assumption 2.1.a (corresponding to $R_l$). □

We now proceed to the proof of the Theorem. We will bound the weak error between random variable $\mathbf{X}^N = \mathbf{X}^N_L$, obtained from micro-macro Algorithm 3.10, and the true solution $\mathbf{X}(T) = \mathbf{X}(T; t^0, \mathbf{X}^0)$ of (1.1) in three steps. In the first part, we derive a recursion for the error at time $t^n = t^{n,0}$, $n = 1, \dots, N$. In the second, we bound the local truncation error. Finally, in the third part we gather the estimates to obtain (3.12).

**Part 1.** Let us fix $g \in C_P^{2(p+1)}(G,\mathbb{R})$ and $L \in \mathbb{N}$. From Assumption 2.1.c we have

$$\begin{aligned}\left|\mathbb{E}g(\mathbf{X}^N) - \mathbb{E}g(\mathbf{X}(T))\right| &\le \sum_{n=1}^{N} \left|\mathbb{E}g\big(\mathbf{X}(T;t^n,\mathbf{X}^n)\big) - \mathbb{E}g\big(\mathbf{X}(T;t^{n-1},\mathbf{X}^{n-1})\big)\right| \\ &\le C_{g,T} \sum_{n=1}^{N} \left|\mathbb{E}g\big(\mathbf{X}^n\big) - \mathbb{E}g\big(\mathbf{X}(t^n;t^{n-1},\mathbf{X}^{n-1})\big)\right|. \end{aligned} \tag{5.2}$$

Here we used the identity $\mathbf{X}(T;t^{n-1},\mathbf{X}^{n-1}) = \mathbf{X}(T;t^n,\mathbf{X}(t^n;t^{n-1},\mathbf{X}^{n-1}))$. The terms in the last sum of (5.2) are exactly the errors produced by one step of the micro-macro acceleration method when there is no initial error, i.e., they are the local truncation errors.

**Part 2.** Let us now fix $n \in \{1,\dots,N\}$ and estimate a single term in the righthand side of (5.2). Recall that Algorithm 3.10 first computes an intermediate solution $\mathbf{X}^{n-1,K}$ by performing $K$ steps of the microscopic scheme at times $t^{n,k}$ $(k = 1,\dots,K)$, and starting from $\mathbf{X}^{n-1}$ at time $t^{n-1} = t^{n-1,0}$ (see (3.9)). Hence we split

$$\begin{aligned}\mathbb{E}g\big(\mathbf{X}^n\big) - \mathbb{E}g\big(\mathbf{X}(t^n;t^{n-1},\mathbf{X}^{n-1})\big) &= \mathbb{E}g\big(\mathbf{X}^n\big) - \mathbb{E}g\big(\mathbf{X}(t^n;t^{n-1,K},\mathbf{X}^{n-1,K})\big) + \\ &+ \mathbb{E}g\big(\mathbf{X}(t^n;t^{n-1,K},\mathbf{X}^{n-1,K})\big) - \mathbb{E}g\big(\mathbf{X}(t^n;t^{n-1},\mathbf{X}^{n-1})\big), \end{aligned} \tag{5.3}$$

and use Lemmas 2.5 (with $s = t^n$) and 5.1 together with $K\delta t \le \Delta t$ to get

$$\left|\mathbb{E}g\big(\mathbf{X}(t^n;t^{n-1,K},\mathbf{X}^{n-1,K})\big) - \mathbb{E}g\big(\mathbf{X}(t^n;t^{n-1},\mathbf{X}^{n-1})\big)\right| \le \bar{C}_{L,T}\Delta t(\delta t)^{p_S} \tag{5.4}$$

with constant $\bar{C}_{L,T}$ depending also on $\mathbf{X}^0$. To estimate the first summand in (5.3) we further split

$$\begin{aligned}\mathbb{E}g\big(\mathbf{X}^n\big) - \mathbb{E}g\big(\mathbf{X}(t^n;t^{n-1,K},\mathbf{X}^{n-1,K})\big) &= \mathbb{E}g\big(\mathbf{X}^n\big) - \mathbb{E}g\big(\mathcal{P}_L(\widetilde{\mathbf{m}}^n,\mathbf{X}^{n-1,K})\big) + \\ &+ \mathbb{E}g\big(\mathcal{P}_L(\widetilde{\mathbf{m}}^n,\mathbf{X}^{n-1,K})\big) - \mathbb{E}g\big(\mathbf{X}(t^n;t^{n-1,K},\mathbf{X}^{n-1,K})\big), \end{aligned}$$

where $\widetilde{\mathbf{m}}^n = \mathcal{R}_L\mathbf{X}(t^n;t^{n-1,K},\mathbf{X}^{n-1,K})$. Using (3.6) in Property 3.8, the second term can be estimated as follows

$$\left|\mathbb{E}g\big(\mathcal{P}_L(\widetilde{\mathbf{m}}^n,\mathbf{X}^{n-1,K})\big) - \mathbb{E}g\big(\mathbf{X}(t^n;t^{n-1,K},\mathbf{X}^{n-1,K})\big)\right| \le C_L\Delta t, \tag{5.5}$$

where $C_L$ depends on $g$ and $C_L \to 0$ as $L \to +\infty$. To estimate the first term recall that $\mathbf{X}^n = \mathcal{P}_L(\mathbf{m}^n,\mathbf{X}^{n-1,K})$ where $\mathbf{m}^n$ is obtained via the extrapolation step (3.10). We can use the continuity of the matching operator (Property 3.7) to get

$$\begin{aligned}\left|\mathbb{E}g\big(\mathbf{X}^n\big) - \mathbb{E}g\big(\mathcal{P}_L(\widetilde{\mathbf{m}}^n,\mathbf{X}^{n-1,K})\big)\right| &\le \hat{C}_L\left\|\mathbf{m}^n - \widetilde{\mathbf{m}}^n\right\| \le \\ &\le \hat{C}_L\left\|\mathbf{m}^n - \mathcal{E}\left((\mathcal{R}_L\mathbf{X}(t^{n-1,k};t^{n-1},\mathbf{X}^{n-1}))_{k=0}^K,\delta t,\Delta t\right)\right\| + \\ &+ \hat{C}_L\left\|\mathcal{E}\left((\mathcal{R}_L\mathbf{X}(t^{n-1,k};t^{n-1},\mathbf{X}^{n-1}))_{k=0}^K,\delta t,\Delta t\right) - \widetilde{\mathbf{m}}^n\right\|. \end{aligned} \tag{5.6}$$

Next we apply the continuity of extrapolation, equation (3.8), together with Lemma 2.5 (with functions $R_l$ and $s = t^{n-1,K}$) to the first term on the right hand side to obtain

$$\begin{aligned}\left\|\mathbf{m}^n - \mathcal{E}\left((\mathcal{R}_L\mathbf{X}(t^{n-1,k};t^{n-1},\mathbf{X}^{n-1}))_{k=0}^K,\delta t,\Delta t\right)\right\| &\le \\ &\le \frac{\Delta t}{K\delta t}\left\|\mathcal{R}_L\mathbf{X}^{n-1,K} - \mathcal{R}_L\mathbf{X}(t^{n-1,K};t^{n-1},\mathbf{X}^{n-1})\right\| \le \\ &\le C_{L,T}(1+\mathbb{E}\|\mathbf{X}^{n-1}\|^{\kappa_{L,T}})\Delta t(\delta t)^{p_S} \le \bar{C}_{L,T}\Delta t(\delta t)^{p_S}, \end{aligned} \tag{5.7}$$

where in the last inequality we used Lemma 5.1. For the second term of (5.6) we have

$$\begin{aligned}\left\|\mathcal{E}\left((\mathcal{R}_L\mathbf{X}(t^{n-1,k};t^{n-1},\mathbf{X}^{n-1}))_{k=0}^K,\delta t,\Delta t\right) - \widetilde{\mathbf{m}}^n\right\| &\le \\ \left\|\mathcal{E}\left((\mathcal{R}_L\mathbf{X}(t^{n-1,k};t^{n-1},\mathbf{X}^{n-1}))_{k=0}^K,\delta t,\Delta t\right) - \mathcal{R}_L\mathbf{X}(t^n;t^{n-1},\mathbf{X}^{n-1})\right\| &+ \\ \left\|\mathcal{R}_L\mathbf{X}(t^n;t^{n-1},\mathbf{X}^{n-1})) - \widetilde{\mathbf{m}}^n\right\|. \end{aligned} \tag{5.8}$$

Lemma 5.2 establishes the estimate on the first term on righthand side of (5.8); for the second term we can once more use Lemma 2.5 (with functions $R_l$ and $s = t^n$) together with Lemma 5.1 to get

$$\left\|\mathcal{R}_L\mathbf{X}(t^n; t^{n-1}, \mathbf{X}^{n-1}) - \widetilde{\mathbf{m}}^n\right\| \leq \bar{C}_{L,T}K(\delta t)^{p_S+1} \leq \bar{C}_{L,T}\Delta t(\delta t)^{p_S}.$$

Combining all these estimates, we obtain

$$\left|\mathbb{E}g(\mathbf{X}^n) - \mathbb{E}g\big(\mathbf{X}(t^n; t^{n-1}, \mathbf{X}^{n-1})\big)\right| \leq C_L\Delta t + 3\bar{C}_{L,T}\Delta t(\delta t)^{p_S} + C^{\mathcal{E}}_{L,T}(\Delta t)^2. \tag{5.9}$$

**Part 3.** Using (5.2) and (5.9), we get

$$\begin{aligned}\left|\mathbb{E}\left[g(\mathbf{X}^N) - g(\mathbf{X}(T))\right]\right| &\leq C_{g,T}N\Delta t(C_L + 3\bar{C}_{L,T}(\delta t)^{p_S} + C^{\mathcal{E}}_{L,T}\Delta t)\\ &\leq C_{g,T}T(C_L + 2\bar{C}_{L,T}(\delta t)^{p_S} + C^{\mathcal{E}}_{L,T}\Delta t),\end{aligned}$$

where we used the estimate $N\Delta t \leq T$. To conclude the proof note that $C_{g,T}$ does not depend on $L$, so we can simply absorb the factor $C_{g,T}T$ into the other constants to obtain (3.12).

# 6 Numerical experiments

In this section, we provide numerical illustration in one spatial dimension for the theoretical results obtained above. We first detail the implementation of the matching algorithm in a Monte Carlo setting (Section 6.1), then we illustrate convergence of the matching (Section 6.2) and the accuracy of the complete micro-macro acceleration method (Section 6.3). It will become clear that numerical L2N matching integrates worse within the full method than KLD or L2D based ones. Therefore, for the numerical experiments in Section 6.3 we restrict ourselves only to divergence based matchings.

## 6.1 Numerical implementation of matching

The numerical matching consists of a procedure that computes the estimate of the Lagrange multipliers parametrizing the PDF of the matching operator (derived in Section 4). In Section 6.1.1, we detail the exact formulas used for the various types of matchings in consideration. Here, we assume that the vector of target moments is given, as well as a weighted ensemble of particles from the prior distribution. A complication arises due to the presence of noise, a consequence of the finite size of the ensemble. In Section 6.1.2, we present the *resampling strategy* used to avoid the degeneracy of weights.

### 6.1.1 Computation of Lagrange multipliers

Let $\mathbf{m} \in \mathbb{R}^L$ be a given vector of target moments corresponding to a restriction operator $\mathcal{R}_L$ generated by functions $R_1, \ldots, R_L$. Assume also that we have a weighted ensemble $\mathscr{X}^\pi = (X_j, w_j)_{j=1}^J$ sampled from a prior distribution $\pi$ with support in $G \subset \mathbb{R}$, where $X_j$ is the $j$-th particle and $w_j$ is its normalized weight (all $w_j$ are non-negative and sum to 1). The matching operator is implemented by computing the appropriate Lagrange multipliers $\widehat{\boldsymbol{\lambda}}_{\mathbf{m},\pi}$ that solve the corresponding dual optimization problem, and results in a new weight $w_j(\widehat{\boldsymbol{\lambda}}_{\mathbf{m},\pi})$ for each particle. The integrals in the formulas for the dual objective function, its gradient and Hessian are estimated using the Monte Carlo method and *importance sampling*. More generally, to estimate averages for a given continuous function of interest $g\colon G \to \mathbb{R}$ with respect to a weighted sample $(X_j, w_j(\boldsymbol{\lambda})_{j=1}^J)$, where $\boldsymbol{\lambda}$ is any vector of Lagrange multipliers, we take

$$\widehat{g} = \sum_{j=1}^{J} g(X_j)\, w_j(\boldsymbol{\lambda}).$$

We now give the specific formulas for the three matching operators discussed so far.

*Example* 6.1. In the case of matching with $L^2$ norm, the Newton-Raphson procedure reduces to the appropriate least-squares problem, as described in Section 4.2. Hence, according to

formula (4.6), the approximate Lagrange multipliers are computed as the numerical solution to the linear system of equations

$$H\boldsymbol{\lambda} = (0, \mathbf{m} - \widehat{\mathbf{m}}(\pi)),$$

where $H$ is an $L+1 \times L+1$ (Hessian) matrix with entries given by (4.7) and $\widehat{\mathbf{m}}(\pi)$ is the Monte Carlo estimate of the moment vector of the prior

$$\widehat{m}(\pi)_l = \sum_{j=1}^{J} R_l(X_j) w_j, \quad l = 1, \ldots, L.$$

We can compute the new weights associated with the matched sample as

$$w_j(\boldsymbol{\lambda}) = w_j \cdot \left( \frac{\sum_{l=0}^{L} \lambda_l R_l(X_j)}{\pi(X_j)} + 1 \right).$$

However, we are facing two problems here. First, the non-negativity of these weights is guaranteed only when the assumptions of Lemma 4.1 hold. Second, we need to evaluate the prior distribution at all particle values $X_j$. Since we generally do not have a closed formula for $\pi$, this requires some density estimation (based on, e.g., histograms or kernel densities, see [62]), and can therefore only be done approximately, potentially introducing additional statistical error and/or bias and increasing the time of computation. These complications do not arise with weights of the KLD and L2D based matchings (discussed in the next two examples), which makes them fit better the complete method. ■

*Remark* 6.2. (Averages for L2N based matching) For the numerical illustration in Section 6.2, we employ formula (4.6) directly and represent the average of a function of interest $g\colon G \to \mathbb{R}$, with respect to the L2N numerical matching, as

$$\bar{g} = \sum_{l=0}^{L} (\widehat{\boldsymbol{\lambda}}_{\mathbf{m},\pi})_l \int_G g(x) R_l(x) \, \mathrm{d}x + \int_G g(x)\pi(x) \, \mathrm{d}x. \tag{6.1}$$

To compute the estimate $\widehat{g}$, we evaluate $L$ deterministic integrals in the sum numerically and estimate the last integral using importance sampling with prior ensemble $\mathscr{X}^{\pi}$. ■

For the matchings based on $f$-divergences, the approximate Lagrange multipliers are obtained via Newton-Raphson iteration applied to (4.19), with the additional constraint $\int_G R_0(x)\phi(x)\,\mathrm{d}x = 1$, where $R_0 \equiv 1$.

*Example* 6.3. For the matching based on KLD, one step of the Newton-Raphson iteration is given as

$$\boldsymbol{\lambda}^{\text{new}} = \boldsymbol{\lambda}^{\text{old}} - \left( \widehat{\nabla^2 D}(\boldsymbol{\lambda}^{\text{old}}) \right)^{-1} \widehat{\nabla D}(\boldsymbol{\lambda}^{\text{old}}),$$

where (see Appendix B) the Monte Carlo estimates of the gradient and Hessian of the objective function $D$ at point $\boldsymbol{\lambda} \in \mathbb{R}^{L+1}$ are for $k, l = 0, \ldots, L$ given by

$$\widehat{\nabla D}(\boldsymbol{\lambda})_l = m_l - \sum_{j=1}^{J} R_l(X_j) w_j(\boldsymbol{\lambda})$$

$$\widehat{\nabla^2 D}(\boldsymbol{\lambda})_{k,l} = -\sum_{j=1}^{J} R_k(X_j) R_l(X_j) w_j(\boldsymbol{\lambda})$$

with weights

$$w_j(\boldsymbol{\lambda}) = w_j \cdot \exp\left( \sum_{l=0}^{L} \lambda_l R_l(X_j) \right) \quad j = 1, \ldots, J.$$ ■

*Example* 6.4. For matching based on L2D the Lagrange multipliers, according to Appendix B, are computed as

$$\boldsymbol{\lambda}^{\text{new}} = \left(\widehat{\nabla^2 D}(\boldsymbol{\lambda}^{\text{old}})\right)^{-1} \left(\mathbf{m} - \widehat{\mathbf{m}}(\boldsymbol{\lambda}^{\text{old}})\right),$$

where, with the (non-negative) weights

$$w_j(\boldsymbol{\lambda}) = w_j \cdot \max\left\{0, \sum_{l=0}^{L} \lambda_l R_l(X_j) + 1\right\}, \quad j = 1, \dots, J,$$

and with $\operatorname{sgn}(0) = 0$ and $\operatorname{sgn}(c) = 1$ for $c > 0$, the Hessian estimate is given by

$$\widehat{\nabla^2 D}(\boldsymbol{\lambda})_{k,l} = -\sum_{n=1}^{J} R_k(X_j) R_l(X_j)\, w_j \operatorname{sgn}(w_j(\boldsymbol{\lambda})), \quad k, l = 0, \dots, L.$$

Here $\widehat{\mathbf{m}}(\boldsymbol{\lambda})$ is the Monte Carlo estimate of the moment vector corresponding to the prior density $\pi$ restricted to the set $\{x : \sum_{l=1}^{L} \lambda_l R_l(x) + 1 \geq 0\}$, i.e,

$$\widehat{\mathbf{m}}(\boldsymbol{\lambda})_l = \sum_{j=1}^{J} R_l(X_j)\, w_j \operatorname{sgn}(w_j(\boldsymbol{\lambda}))$$

for $l = 0, \dots, L$. ■

To sum up, as estimator for the matching $\mathcal{P}_L(\mathbf{m}, \pi)$ we use the vector $\widehat{\boldsymbol{\lambda}}_{\mathbf{m},\pi} = \widehat{\boldsymbol{\lambda}}(\mathbf{m}, \mathscr{X}^{\pi})$ of $L+1$ Lagrange multipliers obtained from the Newton-Raphson procedure. The iteration is stopped when the gradient of the objective function becomes smaller than a fixed value. This vector depends deterministically on the (stochastic) ensemble $\mathscr{X}^{\pi}$ we use to discretize the prior distribution and on the (stochastic) vector $\mathbf{m}$ of target moments.

### 6.1.2 Resampling

The numerical matching associates new weights with the particles in the ensemble corresponding to the prior distribution. However, as the variance of new weights tends to increase, this may result in a degeneracy of the matched ensemble – the weights of a few particles may become very large, while the others become small – leading to large statistical errors in the estimates. To measure degeneracy we will use the divergence (relative entropy) between the new weights $w_j(\widehat{\boldsymbol{\lambda}}_{\mathbf{m},\pi})$ and the uniform weights, all equal to $1/J$, (cf. [47, Ch. 6.1.2.1]) computed as

$$\sum_{j=1}^{J} w_j(\widehat{\boldsymbol{\lambda}}_{\mathbf{m},\pi}) \ln\left(J w_j(\widehat{\boldsymbol{\lambda}}_{\mathbf{m},\pi})\right) \in [0, \ln(J)], \quad \text{for KLD based matching,}$$

$$\frac{1}{J}\sum_{j=1}^{J} \left(J w_j(\widehat{\boldsymbol{\lambda}}_{\mathbf{m},\pi}) - 1\right)^2 \in \left[0, \frac{(J-1)^2}{J}\right], \quad \text{for L2D based matching.}$$

When the divergence of the new weights is larger than a chosen threshold $\alpha$, we initiate a *resampling algorithm* (see [47, Ch. 6.1.2.2]) that generates so-called *branching numbers* – random integers $n_j$, $j = 1, \dots, J$, representing the particle duplication count – such that they sum to $J$ and satisfy the unbiasedness condition $\mathbb{E}(n_j \,|\, \{w_1(\widehat{\boldsymbol{\lambda}}_{\mathbf{m},\pi}), \dots, w_1(\widehat{\boldsymbol{\lambda}}_{\mathbf{m},\pi})\}) = J w_j(\widehat{\boldsymbol{\lambda}}_{\mathbf{m},\pi})$. Thus, after resampling, we obtain a new ensemble of particles $(\widetilde{X}_j)_{j=1}^{J}$ with uniform weights $1/J$, in which there are exactly $n_j$ particles equal to $X_j$. In this paper, we employ the *stratified resampling* strategy [15, 19, 29] that generates random numbers

$$u_k = \frac{(k-1) + \widetilde{u}_k}{J}, \quad \widetilde{u}_k \sim U[0, 1),$$

and takes $n_j = \#\left\{u_k : \; u_k \in \left[\sum_{i=1}^{j-1} w_i(\widehat{\boldsymbol{\lambda}}_{\mathbf{m},\pi}), \sum_{i=1}^{j} w_i(\widehat{\boldsymbol{\lambda}}_{\mathbf{m},\pi})\right)\right\}$.

## 6.2 Properties of numerical matching

We consider the FENE dumbbell model (2.12) in one space dimension, with constant velocity gradient $\kappa(\cdot) \equiv 2$, Weissenberg number $\mathrm{We} = 1$, and maximal spring length $\gamma = \sqrt{b} = 7$. We discretize in time with the accept-reject Euler-Maruyama scheme (2.15)–(2.16) with time step $\delta t = 2 \cdot 10^{-4}$. The probability space is sampled by $J = 10^5$ independent particles. The initial condition at time $t^0 = 0$ is always the invariant distribution of the same FENE dumbbell model but with zero velocity gradient, i.e., the probability distribution proportional to $\exp(2\mathrm{We}\, U)$ where $U$ is the FENE spring potential (2.11). We plot the evolution of stress and the PDFs in Figure 1. In this model, we initially have a gradual spread of the PDF. From $t \approx 1.0$, a sharp peak develops close to the maximum polymer length $\gamma$. The change in the stress is particularly fast between $t = 0.5$ and $t = 2.5$, and later it slows down while the PDF approaches equilibrium (see also [36]).

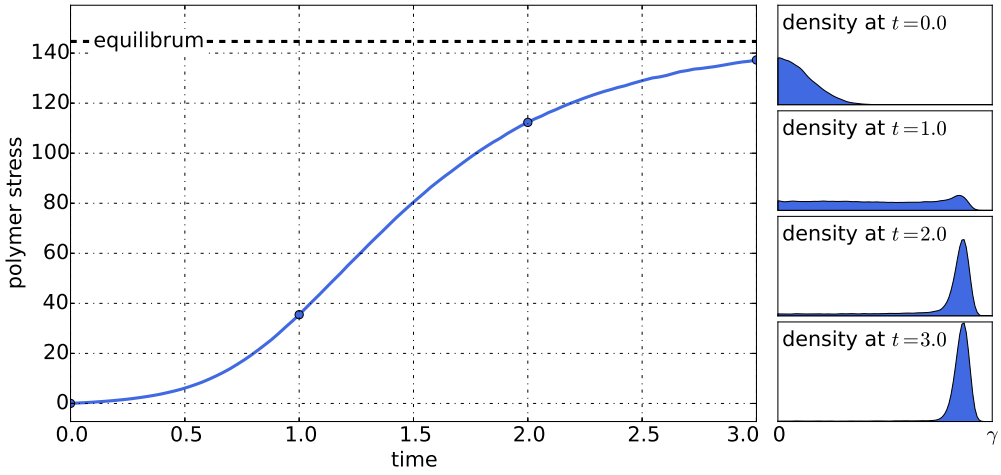


Figure 1: Evolution of polymer stress and the profile of empirical PDFs in the FENE dumbbell model with constant velocity gradient $\kappa = 2.0$ and maximal polymer length $\gamma = 7.0$. The dashed horizontal line denotes the stress in equilibrium.

In the matching, as macroscopic state vector $\mathbf{m} \in \mathbb{R}^L$, we consider the first $L$ normalized even raw moments, corresponding to the restriction operator $\mathcal{R}_L$ generated by the functions $R_l(x) = (x/\gamma)^{2l}$ for $x \in (-\gamma, \gamma)$ and $l = 1, \dots, L$. The Newton-Raphson iteration is stopped when the gradient of an appropriate objective function is smaller than $10^{-9}$. To obtain the *empirical PDFs* corresponding to the ensembles calculated during the simulation, we use *kernel density estimation* with Gaussian kernels [62].

### 6.2.1 Empirical PDFs

In a first experiment, we visually inspect the empirical PDFs obtained from the algorithm for the numerical matching discussed in Section 6.1.1. To this end, we carry out the full microscopic simulation up to time $t^* = 1.1$, and we record the corresponding target ensemble $\mathscr{Y}^*$ and the vector $\mathbf{m}_L^*$ of its first $L$ positive even raw moments, with $L = 3, 5, 7$. As a prior $\mathscr{X}^\pi$, we use the ensemble corresponding to the microscopic simulation at time $t_\pi = 1.0$. Next, we perform the numerical matching with $(\mathbf{m}_L^*, \mathscr{X}^\pi)$ and record the vectors $\widehat{\boldsymbol{\lambda}}_{\mathbf{m}_L^*,\pi}$ for all considered values of $L$. We compare the empirical PDFs of matchings with the ones obtained from prior and target ensembles in Figure 2. We focus on the region where the peak of the density in FENE model forms (see Figure 1).

For L2N based matching, the densities were obtained as the sum of the empirical PDF of $\pi$, based on the ensemble $\mathscr{X}^\pi$, and the (polynomial) functions $(\widehat{\boldsymbol{\lambda}}_{\mathbf{m}_L^*,\pi})^T(R_0, R_1, \dots, R_L)$, where $R_0 \equiv 1$, see equation (6.1). We use formula (4.8) with $\alpha = \max_j\{|X_j^\pi|\}$. The figure visually suggests that increasing the number of moments used for matching makes the approximation of the target PDF more accurate. Moreover, in this example the assumptions

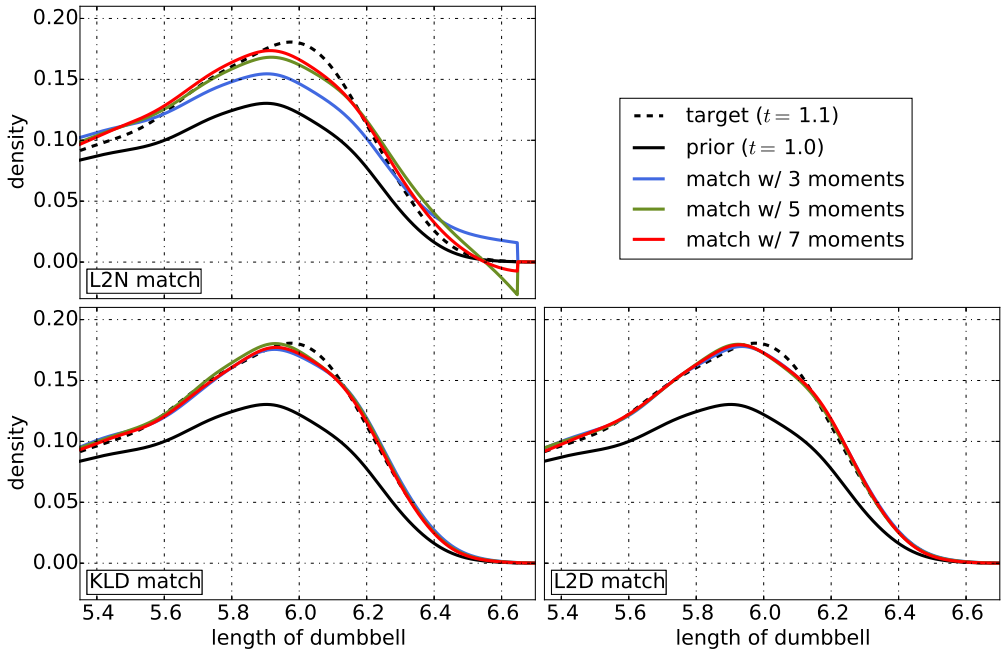


Figure 2: Empirical PDFs of L2N (top left), KLD (bottom left) and L2D (bottom right) based matchings with $L$ moments. The matchings are performed with moments of the target distribution at time $t^* = 1.1$, and prior distribution at time $t_\pi = 1.0$, both taken from microscopic simulation. Computation details are given in Section 6.2.1.

of Lemma 4.1 are not satisfied and the matched density based on L2N can be negative ($L = 5, 7$), even though it is positive for the matching with smaller number of moments ($L = 3$).

The results for the two types of divergence based matchings are presented on the bottom. Here we compute the weights $w_j(\widehat{\boldsymbol{\lambda}}_{\mathbf{m}_L^*,\pi}), j = 1, \ldots, J$ as described in Section 6.1.1, and use the resampling algorithm from Section 6.1.2 combined with kernel density estimation to obtain all empirical PDFs. We see that the target density is approximated more accurately than for L2N based matching even with a small number of moments. The density curves are all similar and are almost indistinguishable on the plot.

### 6.2.2 Error dependence on the number of moments

In the next experiment, we also simulate up to time $t^* = 1.1$ and perform the matching with the moment vector $\mathbf{m}_L^*$, corresponding to the first $L$ even raw moments of the target ensemble at $t^*$ with $L = 3, 5, 7$, and the prior taken from the simulation at time $t_\pi = 1.0$, thus the matching time step $\Delta t$ is $0.1 = 500 \cdot \delta t$. We compute the relative difference between the $l$-th normalized even raw moment $m_l^*$ of the target and the corresponding moment $m_l$ of the matched ensemble: $|m_l^* - m_l|/m_l^*$, for $l = 1, \ldots, 20$. We present the averaged results of 100 i.i.d. experiments with L2N based matching in the left plot of Figure 3, and for both KLD and L2D based matchings in the right plot of Figure 3.

First, note that for $l \leq L$, the relative difference in the moments is below the tolerance of the Newton-Raphson procedure, indicating that, as expected, it converged. Second, for $l > L$, the relative error decreases with increasing $L$. Thus, for the matchings considered here, the error of the moments also decreases for moments that are not constrained during matching.

### 6.2.3 Error dependence on the matching time step

In the next experiment, as previously, we simulate up to time $t^* = 1.1$. We record the prior ensemble $\mathscr{X}^\pi$ at time $t_\pi = 1.0$ and a number of target ensembles for times $t = t_\pi + \Delta t$,

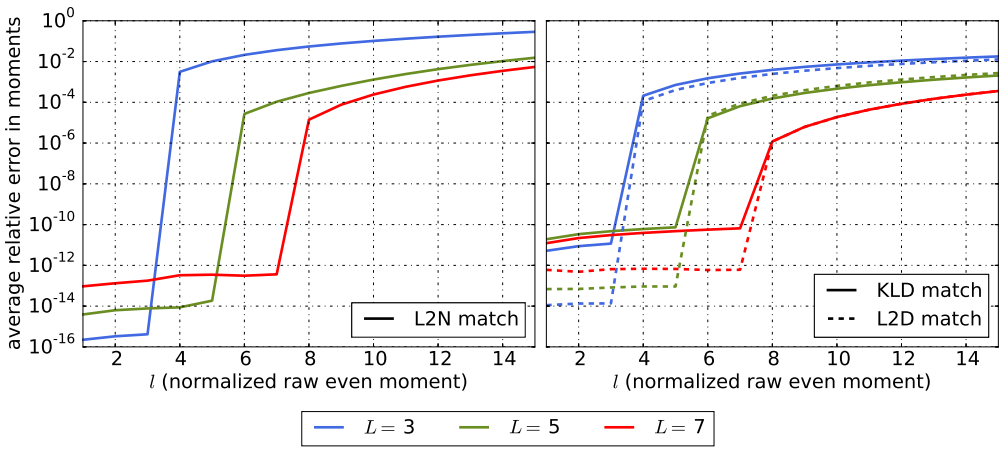


Figure 3: Average relative error of $l$-th moment of L2N (left) and KLD, L2D (right) based matching with $L$ moments as a function of $l$ for 100 i.i.d. runs of the experiment with matching time step $\Delta t = 0.1$. Computation details are given in Section 6.2.2.

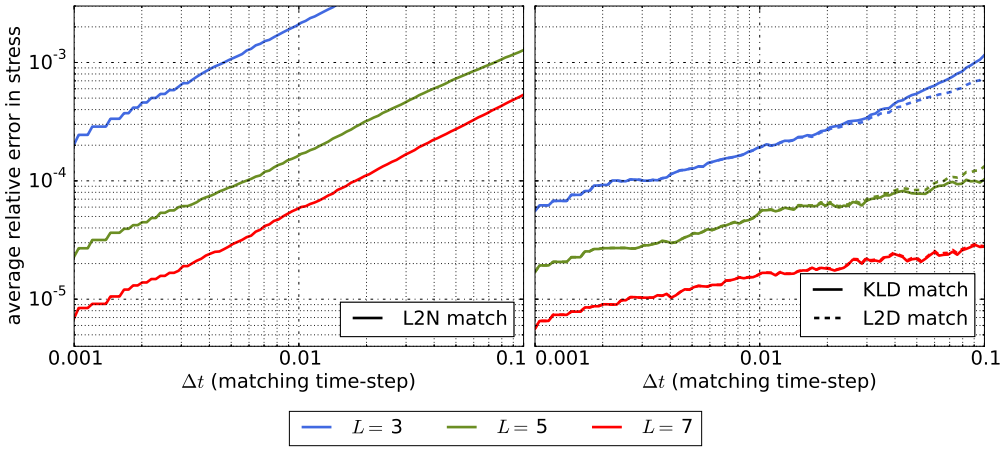


Figure 4: Average relative difference in stress as a function of L2N (left) and KLD, L2D (right) based matching time step for 100 i.i.d. runs of the experiment. Computation details are given in Section 6.2.3.

with $\Delta t \in [5 \cdot \delta t,\, 500 \cdot \delta t]$, where $\delta t = 2 \cdot 10^{-4}$ is the microscopic time step. Then, we perform matchings with moment vectors $\mathbf{m}_L(t)$, corresponding to the first $L = 3, 5, 7$ normalized even raw moments of the target ensemble at time $t$, and the prior. We compute the stress tensor $\widehat{\tau}_p(t)$ of the matching at time $t$ and record the relative difference $|\tau_p(t) - \widehat{\tau}_p(t)|/\tau_p(t)$, where $\tau_p(t)$ is the stress tensor of the corresponding target.

The averaged results of this experiment for 100 i.i.d. runs are presented in Figure 4. We indeed see the linear increase of the matching error as the function of $\Delta t$. Notice also that, as already observed in two previous experiments, the matching error decreases with increasing $L$. From these two figures we can also see that the two divergence based matchings give the same accuracy for modest $\Delta t$ and are significantly better than L2N based matching.

#### 6.2.4 Dependence of Newton-Raphson iteration on the matching time step

In the last experiment, we compare the performance of the optimization procedure for the divergence based matchings. To this end, we record the number of iterations of the Newton-Raphson procedure needed in the previous experiment for each matching time step. We compute the average over all runs of the experiment.

For KLD based matching, the average number of iterations increases with increasing matching time step $\Delta t$ and ranges between 2 and 4 in the considered range of time steps. Moreover, the number of iterations increases monotonically with increasing number of moments used. For L2D based matching we didn't observe any such dependence on $\Delta t$ or the number of moments in this regime. The optimization procedure converges almost always within only one iteration.

## 6.3 Performance of micro-macro acceleration algorithm

In this section, we provide numerical results for the full micro-macro acceleration algorithm 3.10 by performing a simulation of the microscopic FENE dumbbell model with a time-dependent periodic velocity gradient $\kappa$. Hence, we consider equation (2.12) in one space dimension with Weissenberg number $\mathrm{We} = 1$ and maximal spring length $\gamma = \sqrt{b} = 7$. As the velocity field we choose

$$\kappa(t) = 2 \cdot \big(1.1 + \sin(\pi t)\big).$$

For the microscopic simulation, we discretize in time using the accept-reject Euler-Maruyama scheme (2.15)-(2.16), with time step $\delta t = 2 \cdot 10^{-4}$, and in probability space with $J = 10^4$ initial i.i.d. particles sampled from the invariant distribution of equation (2.12) for $\kappa \equiv 0$. During the extrapolation, based on the projective forward Euler method (see Section 3.2), we use the first $L$ normalized even raw moments, corresponding to the restriction operator $\mathcal{R}_L$ generated by the functions $R_l(x) = (x/\gamma)^{2l}$ for $x \in (-\gamma, \gamma)$ and $l = 1, \dots, L$. In all cases we perform $K = 1$ microscopic steps before extrapolation. To restart the microscopic simulation, we use KLD based numerical matching combined with the resampling strategy (described in Section 6.1.2). We set the degeneracy threshold $\alpha = \ln(J)/10$ and check the entropy of the weights each 10 macroscopic time steps.

### 6.3.1 Matching failure and adaptive time stepping

During the simulation the distributions may evolve, for some period of time, on timescales that are similar to those of the macroscopic functions of interest. In that case, when taking a large macroscopic time step, the extrapolated macroscopic state differs significantly from the last available one and can even fall outside of the domain of the matching operator (cf. Remark 3.5). Numerical matching of the prior ensemble with such macroscopic state results in a large number of Newton-Raphson iterations or even the lack of convergence. This "failure" in the matching indicates the need to decrease the extrapolation time step. Consequently, we set a maximal number of Newton-Raphson iterations (as described in Section 6.1.1) and consider the matching to fail if the optimization procedure does not reach the desired tolerance within the given number of iterations. In our experiments, we set the maximal number of Newton-Raphson steps to five.

Based on this observation, we propose the following criterion to adaptively determine the macroscopic step size $\Delta t$. If the matching fails, we reject the step and try again with a time step

$$\Delta t_{\mathrm{new}} = \max(\underline{\alpha}\Delta t, K\delta t), \quad \underline{\alpha} < 1,$$

whereas, when matching succeeds, we accept the step and propose

$$\Delta t_{\mathrm{new}} = \min(\overline{\alpha}\Delta t, \Delta t_{\max}), \quad \overline{\alpha} > 1$$

for the next step. If the macroscopic step size $\Delta t_{\mathrm{new}} = K\delta t$, there is no extrapolation and matching becomes trivial (the identity operator). When this happens, the criterion will ensure that larger time steps are tried after the next burst of microscopic simulation. In the numerical experiments we use $\underline{\alpha} = 0.5$ and $\overline{\alpha} = 1.2$. This choice results in rapid decrease when matching fails and gradual increase when it succeeds.

### 6.3.2 Error dependence on the number of moments

In the first experiment, we use $\Delta t_{\max} = 0.001 = 5.0 \cdot \delta t$ and vary the number $L$ of macroscopic state variables. We simulate up to time $T = 6$. The results of 50 i.i.d. runs of this experiment with $L = 2, 3, 4$ are presented in Figure 5. We make two observations.

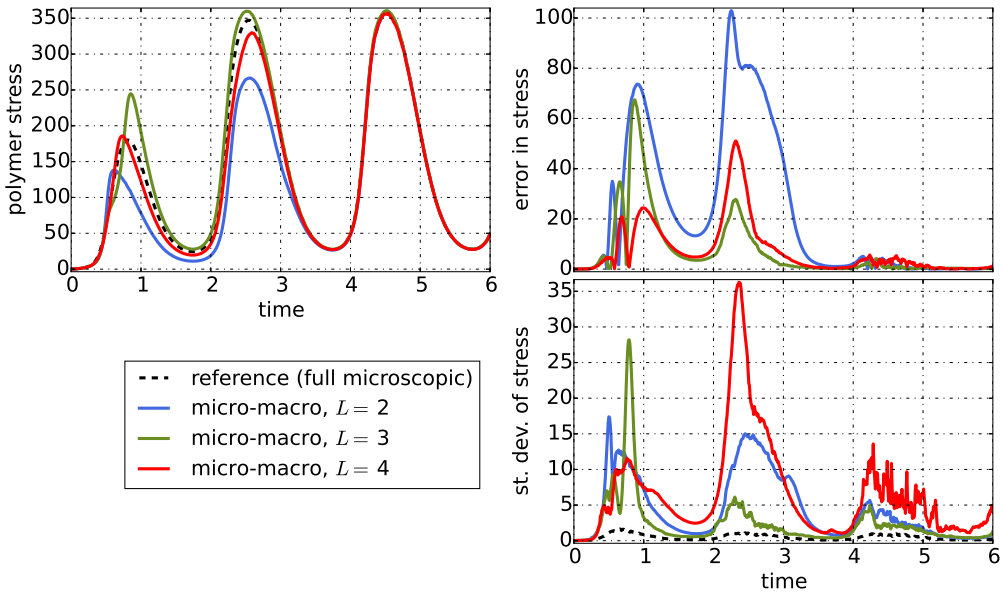


Figure 5: Evolution of the average stress, its absolute error with respect to the reference simulation and the standard deviation for micro-macro simulation with $L$ normalized even raw moments and KLD based matching. Results based on 50 i.i.d. runs of the experiment.

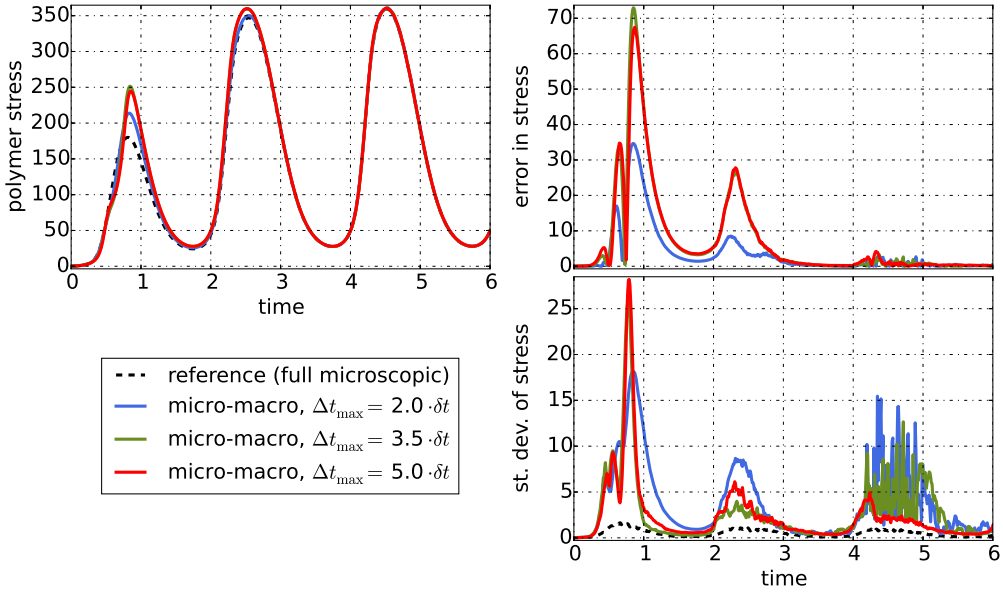
polymer stress
time
error in stress
st. dev. of stress
time
reference (full microscopic)
micro-macro, $\Delta t_{\max} = 2.0 \cdot \delta t$
micro-macro, $\Delta t_{\max} = 3.5 \cdot \delta t$
micro-macro, $\Delta t_{\max} = 5.0 \cdot \delta t$

Figure 6: Evolution of the average stress, its absolute error with respect to the reference simulation and the standard deviation for micro-macro simulation with 3 normalized even raw moments and KLD based matching. Results based on 50 i.i.d. runs of the experiment.

First, the deterministic error decreases with increasing $L$, whereas this tendency is not present in the sample standard deviation. The large variability of the standard deviation, especially for $L = 4$, stems from the ill-posedness of the Hessian matrices used in the Newton-Raphson procedure. Second, we see that the error of the micro-macro acceleration algorithm with respect to the reference simulation decreases as a function of time, and vanishes when the simulation reaches a periodic regime in the third cycle. This behavior can be attributed

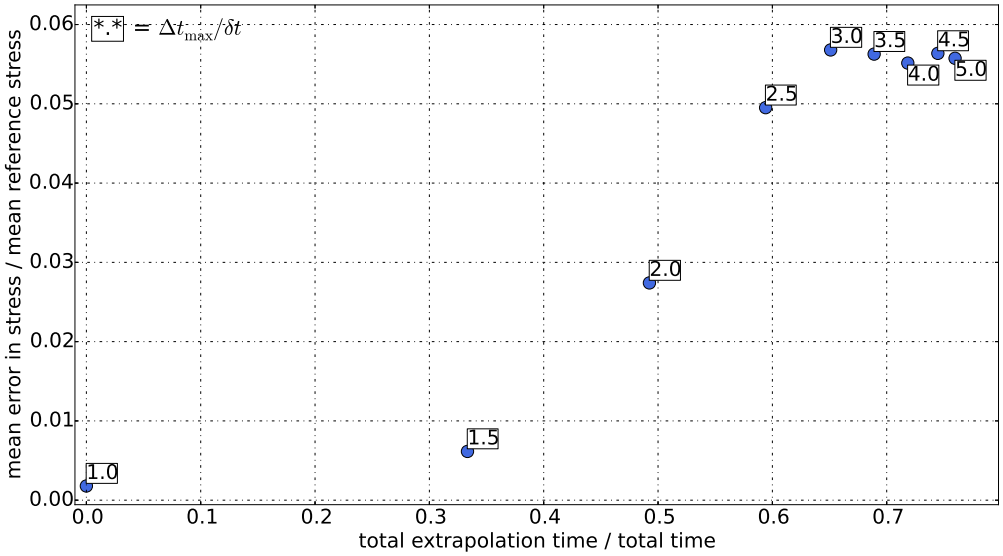


Figure 7: Ratio of time-averaged error in stress to time-averaged reference stress vs percent of extrapolation time for different values of macroscopic time step in the micro-macro simulation with 3 normalized even raw moments. Results based on 50 i.i.d. runs of the experiment.

to the fact that the macroscopic behavior of the system on long time scales is determined by only a few macroscopic state variables.

#### 6.3.3 Error dependence on the macroscopic time step

In the second experiment, we fix $L = 3$ and vary $\Delta t_{\max}$. Figure 6 shows the results for 50 independent runs. While the deterministic error grows with increasing $\Delta t_{\max}$, the adaptive time stepping prevents it from becoming too large and thus we do not see a significant difference between $\Delta t_{\max} = 3.5 \cdot \delta t$ and $5.0 \cdot \delta t$. The righthand plots illustrate the decrease of the error and sample standard deviation as a function of time. However, for small time steps the variability can still be significant at later times (bottom right plot) due to a large number of matchings that need to be performed and that require solving ill-posed problems. Large $\Delta t_{\max}$ reduces this number, especially for larger times where we observed that extrapolation works the best.

To examine the performance of the method for larger numbers of macroscopic time steps we plot in Figure 7 the relation between the mean error and the percent of extrapolation in the time range. On the $y$-axis we present the ratio of the average value over time of the error in stress to the average value over time of stress in a full microscopic simulation. On the $x$-axis we plot the ratio of the time domain covered with extrapolation, computed as $\sum(\Delta t_i - K\delta t)$ with sum over all macroscopic steps in the simulation, to the total time range $T = 6$. For a given $\Delta t_{\max}$, if all macroscopic time steps were equal to $\Delta t_{\max}$, the percent of extrapolation would be $(m-1)/m$, where $m = \Delta t/\delta t$. For $m = 1.5, 2.0, 2.5$ the $x$-coordinates of corresponding points on the plot are close to this maximum, meaning the simulation was performed with maximal extrapolation step for almost all times. For higher ratios $m$ this is no longer the case and we can see the effects of the adaptive time-stepping that makes the points clump together in the top right corner of the Figure.

## 7 Conclusions and outlook

We presented and analyzed a micro-macro acceleration technique for the Monte Carlo simulation of stochastic differential equations (SDEs), in which short bursts of simulation using an ensemble of microscopic SDE realizations are combined with an extrapolation of an

estimated macroscopic state forward in time. The method is designed for problems in which the required time step for each realization of the SDE is small compared to the time scales on which the function of interest evolves. We proved (rigorously) that the proposed procedure converges in the absence of statistical error provided the matching operator satisfies a number of natural conditions. We introduced a matching operator based on the $L2$-norm that satisfies these conditions and illustrated the behavior of the method numerically, also for matching operators based on $f$-divergences.

In future work, we will perform a more detailed study of the matching operators based on $f$-divergences and investigate stability and propagation of statistical error on long time scales. From an algorithmic point of view, this work raises questions on the adaptive/automatic selection of all method parameters (number of moments to extrapolate, macroscopic time step, number of SDE realizations) to ensure a reliable computation with minimal computational cost. Also, a numerical comparison with other approaches, such as implicit approximations, could be envisaged.


## Acknowledgements

This work was partially supported by the Research Council of the University of Leuven through grant OT/13/66, by the Interuniversity Attraction Poles Programme of the Belgian Science Policy Office under grant IUAP/V/22, and by the Research Foundation – Flanders (FWO – Vlaanderen) under grant G.A003.13. The computational resources and services used in this work were provided by the VSC (Flemish Supercomputer Center), funded by the Hercules Foundation and the Flemish Government – department EWI. The scientific responsibility for this work rests with its authors.


## A Convex optimization with integral functionals

Our divergence matching operators are defined using an optimization problem with an integral operator given by the convex function $f\colon [0,+\infty) \to (-\infty,+\infty]$. The *effective domain* of $f$ is defined as $\operatorname{eff\,dom} f = \{t \in \mathbb{R} :\ f(t) < +\infty\}$. Let $\widetilde{\mathbf{m}} \in \mathbb{R}^{L+1}$ and consider the following *primal (entropy) problem* in $L^p(G,\mu)$

$$(EP)_p \qquad \begin{cases} \inf & \mathcal{I}_f(\phi) = \displaystyle\int_G f(\phi(\mathbf{x}))\ \mathrm{d}\mu(\mathbf{x}) \\ \text{subject to} & \widetilde{\mathcal{R}}_L\phi = \widetilde{\mathbf{m}}, \\ & \phi \in L^p_+(G,\mu), \end{cases}$$

where $\widetilde{\mathcal{R}}_L\colon L^p(G,\mu) \to \mathbb{R}^{L+1}$ is a linear operator generated by functions $R_l \in L^q(G,\mu)$, $l = 0,\dots,L$ (cf. (4.1)). The mapping $\mathcal{I}_f$ is a well-defined convex functional on $L^p(G,\mu)$ with values in $(-\infty,+\infty]$ as long as $f$ is a lower semi-continuous proper convex function (see [56, Lem. 1 and Thm. 1]). We say that $(EP)_p$ is *consistent* if there exists a function $\phi \in L^p_+(G,\mu)$ such that $\widetilde{\mathcal{R}}_L\phi = \widetilde{\mathbf{m}}$ and $\mathcal{I}_f(\phi) < +\infty$. To compute the primal optimal we consider the corresponding unconstrained (at least formally) *Lagrangian dual problem*

$$(DEP)_p \qquad \begin{cases} \sup & D(\boldsymbol{\lambda}) = \widetilde{\mathbf{m}}^T\boldsymbol{\lambda} - \displaystyle\int_G f_+^*\left(\widetilde{\mathcal{R}}_L^T\boldsymbol{\lambda}(\mathbf{x})\right)\ \mathrm{d}\mu(\mathbf{x}) \\ \text{subject to} & \boldsymbol{\lambda} \in \mathbb{R}^{L+1}. \end{cases}$$

Here the function $f_+$, defined as being equal to $f$ on $[0,+\infty)$ and to $+\infty$ on $(-\infty,0)$, encodes the non-negativity constraint from the primal problem. The *(convex) conjugate* $f_+^*\colon \mathbb{R} \to \mathbb{R}$ is given by

$$f_+^*(s) = \sup_{t\geq 0}\{s\cdot t - f(t)\}. \tag{A.1}$$

The *transpose* $\widetilde{\mathcal{R}}_L^T\colon \mathbb{R}^{L+1} \to L^q(G,\mu)$ of $\widetilde{\mathcal{R}}_L$, defined with relation $\langle \widetilde{\mathcal{R}}_L^T \boldsymbol{\lambda},\, \phi\rangle = (\widetilde{\mathcal{R}}_L \phi)^T \cdot \boldsymbol{\lambda}$, satisfies

$$\widetilde{\mathcal{R}}_L^T \boldsymbol{\lambda} = \sum_{l=0}^{L} \lambda_l R_l, \quad \boldsymbol{\lambda} \in \mathbb{R}^{L+1}. \tag{A.2}$$

We call $D$ the *dual objective function* and each solution $\overline{\boldsymbol{\lambda}} \in \mathbb{R}^{L+1}$ to $(DEP)_p$ is referred to as *dual optimal*.

Let us state here the main result we use to analyze the matching operators in Section 4. This theorem is a particular case of [4, Thm. 4.8.]. Recall that a finite set of measurable functions on $G$ is called *pseudo-Haar* if the functions are linearly independent on every non-null subset of $G$. For example, a finite collection of analytic and linearly independent functions on $G$ is pseudo-Haar [4, Prop. 2.8].

**Theorem A.1.** *Let $1 \le p < +\infty$ and suppose that the integrand $f\colon \mathbb{R} \to (-\infty, +\infty]$ is lower semi-continuous and strictly convex on $\operatorname{eff\,dom} f \supset [0, +\infty)$, and is superlinear at $+\infty$, i.e. $\lim_{t\to+\infty} f(t)/t = +\infty$. If, in addition, the moment functions $R_l$, $l = 1, \dots, L$, are pseudo-Haar and for $\widetilde{\mathbf{m}} = (m_0, \dots, m_L) \in \mathbb{R}^{L+1}$ it holds*

$$\widetilde{\mathbf{m}} \in \operatorname{int} \widetilde{\mathcal{R}}_L \left( L^p_+(G,\mu) \right), \tag{A.3}$$

*the primal problem $(EP)_p$ is consistent, the primal and dual optimal values are the same, the dual optimal value is attained, and the unique primal solution is given by*

$$\overline{\phi} = (f_+^*)' \left( \sum_{l=0}^{L} \overline{\lambda}_l R_l \right), \tag{A.4}$$

*where $\overline{\boldsymbol{\lambda}} = (\overline{\lambda}_0, \dots, \overline{\lambda}_L) \in \mathbb{R}^{L+1}$ is the dual optimal.*

See also [4, Thm. 2.9.] for the explanation how the pseudo-Haar property of moment functions is useful to ensure the consistency of the primal problem. Since $f$ is lower semi-continuous and superlinear at $+\infty$, the mapping $t \mapsto st - f(t)$ is, for each $s$, upper semi-continuous and bounded from above on $[0, +\infty)$. This implies that the supremum in (A.1) is attained, thus $f_+^*(s) < +\infty$ for all $s$, and in consequence $\operatorname{eff\,dom} f_+^* = \mathbb{R}$. Moreover, assumptions (1) and (2) guarantee that the conjugate function $f_+^*$ is differentiable on the interior of its domain, see [4, Thm. 4.6.], so the right-hand side of (A.4) is well-defined.

As a consequence of (A.4), we get the formula for the gradient of the dual objective function in $(DEP)_p$

$$\nabla D(\boldsymbol{\lambda}) = \left[ \widetilde{\mathbf{m}} - \widetilde{\mathcal{R}}_L \left( (f_+^*)'(\widetilde{\mathcal{R}}_L^T \boldsymbol{\lambda}) \right) \right]^T, \quad \boldsymbol{\lambda} \in \mathbb{R}^{L+1}. \tag{A.5}$$

Hence, due to concavity of $D$, the dual optimal $\overline{\boldsymbol{\lambda}}$ can be calculated as the unique vector that satisfies $\nabla D(\overline{\boldsymbol{\lambda}}) = 0$.

# B Newton-Raphson procedures for matching

**Kullback-Leibler** We now present the derivation of the Newton-Raphson method to solve the system (4.22). From (A.5) we already know the gradient of the dual optimal function, which in this case is given by

$$\nabla D(\lambda)_l = m_l - \int_G R_l(\mathbf{x}) \exp\left( \sum_{i=0}^{L} \lambda_i R_i(\mathbf{x}) \right) \pi(\mathbf{x})\, \mathrm{d}\mathbf{x}, \quad l = 0, \dots, L. \tag{B.1}$$

Hence the $k, l$ component of the Hessian is

$$\begin{aligned}\nabla^2 D(\lambda)_{k,l} &= -\partial_{\lambda_k} \int_G R_l(\mathbf{x}) \exp\left(\sum_{i=0}^{L} \lambda_i R_i(\mathbf{x})\right) \pi(\mathbf{x})\ \mathrm{d}\mathbf{x} \\ &= -\int_G R_k(\mathbf{x}) R_l(\mathbf{x}) \exp\left(\sum_{i=0}^{L} \lambda_i R_i(\mathbf{x})\right) \pi(\mathbf{x})\ \mathrm{d}\mathbf{x}, \quad k, l = 0, \dots, L. \end{aligned} \tag{B.2}$$

Since, for fixed $\mathbf{x} \in G$, the function $\lambda_k \mapsto R_l(\mathbf{x}) \exp\left(\sum_{i=0}^{L} \lambda_i R_i(\mathbf{x})\right)$ is continuously differentiable, and for every $\delta > 0$ the function

$$\mathbf{x} \mapsto \sup_{\Theta \in [-\delta, \delta]} |R_k(\mathbf{x}) R_l(\mathbf{x})| \exp\left(\sum_{i=0}^{L} \lambda_i R_i(\mathbf{x}) + \Theta\right)$$

is integrable with respect to $\pi\, \mathrm{d}\mathbf{x}$, the interchangeability of integration and differentiation in (B.2) is justified by [16, Thm. A.5.2.]. To sum up, the Newton-Raphson iteration to determine the approximation of dual optimal $\overline{\boldsymbol{\lambda}} \in \mathbb{R}^{L+1}$ for the matching with KLD, i.e. solving (4.22), is

$$\boldsymbol{\lambda}^{\text{new}} = \boldsymbol{\lambda}^{\text{old}} - \left(\nabla^2 D(\boldsymbol{\lambda}^{\text{old}})\right)^{-1} \nabla D(\boldsymbol{\lambda}^{\text{old}}) \tag{B.3}$$

where the gradient and the Hessian of the objective function are given by (B.1) and (B.2) respectively.

**$L^2$ divergence** We now present the derivation of the Newton-Raphson method to solve the system (4.25). Note that we can write

$$\begin{aligned}\int_G R_l(\mathbf{x}) \max\left(0, \sum_{k=0}^{L} \lambda_k R_k(\mathbf{x})\right) \pi(\mathbf{x})\ \mathrm{d}\mathbf{x} &= \int_{[\boldsymbol{\lambda}^T \mathbf{R} \geq 0]} R_l(\mathbf{x}) \left(\sum_{k=0}^{L} \lambda_k R_k(\mathbf{x})\right) \pi(\mathbf{x})\ \mathrm{d}\mathbf{x} \\ &= \sum_{k=0}^{L} \lambda_k \int_{[\boldsymbol{\lambda}^T \mathbf{R} \geq 0]} R_l(\mathbf{x}) R_k(\mathbf{x})\, \pi(\mathbf{x})\ \mathrm{d}\mathbf{x},\end{aligned}$$

where $[\boldsymbol{\lambda}^T \mathbf{R} \geq 0] = \{\mathbf{x} \in \mathbb{R}^d : \sum_{k=0}^{L} \lambda_k R_k(\mathbf{x}) \geq 0\}$. Similar reasoning as in the previous section reveals that the Hessian of the dual objective function is

$$\nabla^2 D(\boldsymbol{\lambda})_{k,l} = -\int_{[\boldsymbol{\lambda}^T \mathbf{R} \geq 0]} R_l(\mathbf{x}) R_k(\mathbf{x})\, \pi(\mathbf{x})\, \mathrm{d}\mathbf{x}, \quad k, l = 0, \dots, L, \tag{B.4}$$

thus the gradient is given by

$$\nabla D(\boldsymbol{\lambda}) = (1, \mathbf{m}) + \nabla^2 D(\boldsymbol{\lambda}) \boldsymbol{\lambda}. \tag{B.5}$$

The relation between gradient and Hessian of the objective function $D$ in (B.5) simplifies the Newton-Raphson iteration, originally given as in (*B*.3), to

$$\boldsymbol{\lambda}^{\text{new}} = \left(\nabla^2 D(\boldsymbol{\lambda}^{\text{old}})\right)^{-1} (1, \mathbf{m}). \tag{B.6}$$

# References


[1] Abdulle Abdulle, Gilles Vilmart, and Konstantinos C. Zygalakis. Mean-square $A$-stable diagonally drift-implicit integrators of weak second order for stiff Itô stochastic differential equations. *BIT*, 53(4):827–840, 2013.

[2] Sadegh Amiri and Seyed Mohammad Hosseini. A class of weak second order split-drift stochastic Runge-Kutta schemes for stiff SDE systems. *J. Comput. Appl. Math.*, 275:27–43, 2015.

[3] Kendall E. Atkinson and Weimin Han. *Theoretical Numerical Analysis*, volume 39. Springer, 3rd edition, 2009.

[4] Jonathan M. Borwein and Adrian S. Lewis. Duality Relationships for Entropy-Like Minimization Problems. *SIAM J. Control Optim.*, 29(2):325–338, 1991.

[5] Evelyn Buckwar and Cónall Kelly. Non-normal drift structures and linear stability analysis of numerical methods for systems of stochastic differential equations. *Comput. Math. Appl.*, 64(7):2282–2293, 2012.

[6] Evelyn Buckwar and Thorsten Sickenberger. A structural analysis of asymptotic mean-square stability for multi-dimensional linear stochastic differential systems. *Appl. Numer. Math.*, 62(7):842–859, 2012.

[7] Russel E. Caflisch. Monte Carlo and quasi-Monte Carlo methods. *Acta Numer.*, 7:1–49, 1998.

[8] Imre Csiszár. Information-type measures of difference of probability distributions and indirect observations. *Studi Sci. Math. Hungarica*, 2:299–318, 1967.

[9] Kristian Debrabant. Runge-Kutta methods for third order weak approximation of SDEs with multidimensional additive noise. *BIT*, 50(3):541–558, 2010.

[10] Kristian Debrabant and Anne Kværnø. B-series analysis of stochastic Runge-Kutta methods that use an iterative scheme to compute their internal stage values. *SIAM J. Numer. Anal.*, 47(1):181–203, 2008/09.

[11] Kristian Debrabant and Anne Kværnø. B-series analysis of iterated Taylor methods. *BIT*, 51(3):529–553, 2011.

[12] Kristian Debrabant and Andreas Rößler. Diagonally drift-implicit Runge-Kutta methods of weak order one and two for Itô SDEs and stability analysis. *Appl. Numer. Math.*, 59(3-4):595–607, 2009.

[13] Kristian Debrabant and Andreas Rößler. Families of efficient second order Runge-Kutta methods for the weak approximation of Itô stochastic differential equations. *Appl. Numer. Math.*, 59(3-4):582–594, 2009.

[14] Kristian Debrabant and Andreas Rößler. On the acceleration of the multilevel Monte Carlo method. *J. Appl. Probab.*, 52(2):307–322, 2015.

[15] Randal Douc, Olivier Cappé, and Eric Moulines. Comparison of resampling schemes for particle filtering. In *ISPA 2005. Proc. 4th Int. Symp. Image Signal Process. Anal. 2005.*, pages 64–69, 2005.

[16] Rick Durrett. *Probability: Theory and Examples.* Cambridge Series in Statistical and Probabilistic Mathematics. Cambridge University Press, 4th edition, 2010.

[17] Weinan E and Bjorn Engquist. The heterogeneous multi-scale methods. *Commun. Math. Sci.*, 1(1):87–132, 2003.

[18] Weinan E, Bjorn Engquist, Xiantao Li, Weiqing Ren, and Eric Vanden-Eijnden. Heterogeneous multiscale methods: a review. *Commun. Comput. Phys.*, 2(3):367–450, 2007.

[19] Mohamed El Makrini, Benjamin Jourdain, and Tony Lelièvre. Diffusion Monte Carlo method: numerical analysis in a simple case. *ESAIM Math. Model. Numer. Anal.*, 41(2):189–213, 2007.

[20] C. William Gear and Ioannis G. Kevrekidis. Projective methods for stiff differential equations: problems with gaps in their eigenvalue spectrum. *SIAM J. Sci. Comput.*, 24(4):1091–1106, 2003.

[21] C. William Gear, Ioannis G. Kevrekidis, and Constantinos Theodoropoulos. 'Coarse' integration/bifurcation analysis via microscopic simulators: micro-Galerkin methods. *Comput. Chem. Eng.*, 26(7-8):941–963, 2002.

[22] Michael B. Giles. Improved multilevel Monte Carlo convergence using the Milstein scheme. In *Monte Carlo and quasi-Monte Carlo methods 2006*, pages 343–358. Springer, Berlin, 2008.

[23] Michael B. Giles. Multilevel Monte Carlo path simulation. *Oper. Res.*, 56(3):607–617, 2008.

[24] Amir Haghighi and S. Mohammad Hosseini. Analysis of asymptotic mean-square stability of a class of Runge-Kutta schemes for linear systems of stochastic differential equations. *Math. Comput. Simulation*, 105:17–48, 2014.

[25] Diego Bricio Hernández and Renato Spigler. *A*-stability of Runge-Kutta methods for systems with additive noise. *BIT*, 32(4):620–633, 1992.

[26] Diego Bricio Hernández and Renato Spigler. Convergence and stability of implicit Runge–Kutta methods for systems with multiplicative noise. *BIT*, 33(4):654–669, 1993.

[27] Markus Herrchen and Hans Christian Öttinger. A detailed comparison of various FENE dumbbell models. *J. Non-Newtonian Fluid Mech.*, 68(1):17–42, 1997.

[28] Desmond J. Higham. Mean-square and asymptotic stability of the stochastic theta method. *SIAM J. Numer. Anal.*, 38(3):753–769 (electronic), 2000.

[29] Jeroen D. Hol, Thomas B. Schön, and Fredrik Gustafsson. On resampling algorithms for particle filters. In *NSSPW - Nonlinear Stat. Signal Process. Work. 2006*, 2006.

[30] Richard B. Holmes. *Geometric Functional Analysis*, volume 24 of *Graduate Texts in Mathematics*. Springer-Verlag, New York Hedelberg Berlin, 1975.

[31] Jiaxing Hong and Ge Yang. On the regularity of solutions to FENE models. *SIAM J. Math. Anal.*, 45(4):2228–2252, 2013.

[32] Yunkyong Hyon, Qiang Du, and Chun Liu. An enhanced macroscopic closure approximation to the micro-macro FENE model for polymeric materials. *Multiscale Model. Simul.*, 7(2):978–1002, 2008.

[33] Patrick Ilg, Iliya V. Karlin, and Hans Christian Öttinger. Canonical distribution functions in polymer dynamics . ( I ). Dilute solutions of flexible polymers. *Physica A*, 315:367–385, 2002.

[34] Benjamin Jourdain and Tony Lelièvre. Mathematical analysis of a stochastic differential equation arising in the micro-macro modelling of polymeric fluids. In *Probabilistic Methods in Fluids*, pages 205–223, 2003.

[35] Benjamin Jourdain, Tony Lelièvre, and Claude Le Bris. Existence of solution for a micro-macro model of polymeric fluid: the FENE model. *J. Funct. Anal.*, 209(1):162–193, apr 2004.

[36] Roland Keunings. On the Peterlin approximation for finitely extensible dumbbells. *J. Non-Newtonian Fluid Mech.*, 68(1):85–100, 1997.

[37] Ioannis G. Kevrekidis, C. William Gear, James M. Hyman, Panagiotis G. Kevrekidis, Olof Runborg, and Constantinos Theodoropoulos. Equation-free, coarse-grained multiscale computation: enabling microscopic simulators to perform system-level analysis. *Commun. Math. Sci.*, 1(4):715–762, 2003.

[38] Ioannis G. Kevrekidis and Giovanni Samaey. Equation-free multiscale computation: algorithms and applications. *Annu. Rev. Phys. Chem.*, 60:321–344, 2009.

[39] Peter E. Kloeden and Eckhard Platen. *Numerical Solution of Stochastic Differential Equations*, volume 23 of *Applications of Mathematics*. Springer Berlin Heidelberg, 1999.

[40] Yoshio Komori. Weak second-order stochastic Runge–Kutta methods for non-commutative stochastic differential equations. *J. Comput. Appl. Math.*, 206(1):158–173, 2007.

[41] Yoshio Komori. Weak first- or second-order implicit Runge-Kutta methods for stochastic differential equations with a scalar Wiener process. *J. Comput. Appl. Math.*, 217(1):166–179, 2008.

[42] Pauline Lafitte, Annelies Lejon, and Giovanni Samaey. eprint arxiv:1404.6104, 4 2014.

[43] Pauline Lafitte, Ward Melis, and Giovanni Samaey. eprint arxiv:1406.4305, 6 2014.

[44] Manuel Laso and Hans Christian Öttinger. Calculation of viscoelastic flow using molecular models: the CONNFFEESSIT approach. *J. Non-Newtonian Fluid Mech.*, 47:1–20, jun 1993.

[45] Claude Le Bris and Tony Lelièvre. Multiscale Modelling of Complex Fluids : A Mathematical Initiation. In *Multiscale Model. Simul. Sci.*, pages 49–137. Springer Berlin Heidelberg, 2009.

[46] Steven L. Lee and C. William Gear. Second-order accurate projective integrators for multiscale problems. *J. Comput. Appl. Math.*, 201:258–274, Jan 2007.

[47] Tony Lelièvre, Mathias Rousset, and Gabriel Stolz. *Free Energy Computations. A Mathematical Perspective*. Imperial College Press, London, 2010.

[48] Gregory Lielens, Pierre Halin, Ingrid Jaumain, Roland Keunings, and Vincent Legat. New closure approximations for the kinetic theory of finitely extensible dumbbells. *J. Non-Newtonian Fluid Mech.*, 76(1-3):249–279, apr 1998.

[49] Gregory Lielens, Roland Keunings, and Vincent Legat. The FENE-L and FENE-LS closure approximations to the kinetic theory of finitely extensible dumbbells. *J. Non-Newtonian Fluid Mech.*, 87(2-3):179–196, 1999.

[50] Hailiang Liu and Jaemin Shin. Global well-posedness for the microscopic FENE model with a sharp boundary condition. *J. Differ. Equ.*, 252(1):641–662, 2012.

[51] Grigori N. Milstein. *Numerical Integration of Stochastic Differential Equations*, volume 313 of *Mathematics and Its Applications*. Springer Netherlands, 1995.

[52] Nigel J. Newton. Variance reduction for simulated diffusions. *SIAM J. Appl. Math.*, 54(6):1780–1805, 1994.

[53] Hans Christian Öttinger. *Stochastic processes in polymeric fluids*. Springer Berlin Heidelberg, 1996.

[54] Grigorios A. Pavliotis. *Stochastic Processes and Applications: Diffusion Processes, the Fokker-Planck and Langevin Equations*, volume 60 of *Texts in Applied Mathematics*. Springer Berlin Heidelberg, 2014.

[55] Ramiro Rico-Martínez, C. William Gear, and Ioannis G. Kevrekidis. Coarse projective kmc integration: forward/reverse initial and boundary value problems. *Journal of Computational Physics*, 196(2):474–489, 2004.

[56] Ralph T. Rockafellar. Integrals which are convex functionals. *Pacific J. Math.*, 24(3):525–539, 1968.

[57] Andreas Rößler. Rooted tree analysis for order conditions of stochastic Runge–Kutta methods for the weak approximation of stochastic differential equations. *Stoch. Anal. Appl.*, 24(1):97–134, 2006.

[58] Andreas Rößler. Second order Runge–Kutta methods for Stratonovich stochastic differential equations. *BIT*, 47(3):657–680, 2007.

[59] Andreas Rößler. Stochastic Taylor Expansions for Functionals of Diffusion Processes. *Stoch. Anal. Appl.*, 28(3):415–429, 2010.

[60] Yoshihiro Saito and Taketomo Mitsui. Stability analysis of numerical schemes for stochastic differential equations. *SIAM J. Numer. Anal.*, 33(6):2254–2267, 1996.

[61] Giovanni Samaey, Tony Lelièvre, and Vincent Legat. A numerical closure approach for kinetic models of polymeric fluids: exploring closure relations for FENE dumbbells. *Comput. Fluids*, 43:119–133, 2011.

[62] Dawid W. Scott. *Multivariate Density Estimation: Theory, Practice, and Visualization.* Wiley Series in Probability and Statistics. Wiley, 2nd edition, 2015.

[63] Renaud Sizaire, Gregory Lielens, Ingrid Jaumain, Roland Keunings, and Vincent Legat. On the hysteretic behaviour of dilute polymer solutions in relaxation following extensional flow. *J. Non-Newtonian Fluid Mech.*, 82(2-3):233–253, may 1999.

[64] Ben P. Sommeijer. Increasing the real stability boundary of explicit methods. *Comput. Math. Appl.*, 19(6):37–49, Jan 1990.

[65] Giorgio Talenti. Recovering a function from a finite number of moments. *Inverse Probl.*, 3:501–517, 1987.

[66] Ángel Tocino. Mean-square stability of second-order Runge–Kutta methods for stochastic differential equations. *J. Comput. Appl. Math.*, 175(2):355–367, 2005.

[67] Ángel Tocino, R. Zeghdane, and Lyazid Abbaoui. Linear mean-square stability analysis of weak order 2.0 semi-implicit Taylor schemes for scalar stochastic differential equations. *Appl. Numer. Math.*, 68:19–30, 2013.

[68] Christophe Vandekerckhove, Ioannis G. Kevrekidis, and Dirk Roose. An efficient Newton–Krylov implementation of the constrained runs scheme for initializing on a slow manifold. *Journal on Scientific Computing*, 39(2):167–188, 2009.

[69] Christophe Vandekerckhove and Dirk Roose. Accuracy analysis of acceleration schemes for stiff multiscale problems. *J. Comput. Appl. Math.*, 211(2):181–200, 2008.

[70] Han Wang, Kun Li, and Pingwen Zhang. Crucial properties of the moment closure model FENE-QE. *Journal of Non-Newtonian Fluid Mechanics*, 150(2-3):80–92, 2008.